Conformational Analyses of Physiological Binary and Ternary Copper(II) Complexes with L-Asparagine and L-Histidine; Study of Tridentate Binding of Copper(II) in Aqueous Solution

Michael Ramek,[a] Marijana Marković,[a] Ilina Mutapčić,[a] Jelena Pejić,[b] Anne-Marie Kelterer,[a] and Jasmina Sabolović*[b]

This study explores the structural properties and energy landscapes of the physiologically important bis(L-asparaginato) copper(II) [Cu(L-Asn)$_2$] and (L-histidinato)(L-asparaginato)copper (II) [Cu(L-His)(L-Asn)]. The conformational analyses in the gas phase and implicitly modeled water medium, and magnetic parameters of electron paramagnetic resonance spectra were attained using density functional theory calculations. The apical Cu^{II} coordination and hydrogen bonding were analyzed. Predicted lower-energy structures enabled the confirmation and, for apical bonding, also the refinement of structural proposals from literature. Available experimental results were indecisive regarding the amido-group binding in the Cu^{II} equatorial plane in solutions, but the examination of the relative stability of Cu(L-Asn)$_2$ conformers in 30 binding modes confirms the glycine-like mode as the most stable one. Previously reported experimental results for Cu(L-His)(L-Asn) were interpreted for L-His to have a tridentate histamine-like mode. However, the aqueous conformers with L-His in the glycinato mode are also predicted to have low energies, which does not contradict the tridentate L-His binding. The predicted magnetic parameters of conformers with an apical oxygen atom (intramolecular or from a water molecule) can reproduce the experimental data. An extent of conformational flexibility and abundance of L-His-containing ternary copper(II) amino acid complexes under physiological conditions may be related.

1. Introduction

Copper is an essential trace element, and a structural and catalytic cofactor in the active sites of many metalloproteins (e.g., superoxide dismutase, tyrosinase, cytochrome c oxidase, ascorbate oxidase).[1,2] The importance of maintaining copper physiological concentrations in healthy organisms became evident in the diseases of genetic origin, traced to malfunctioned copper transport and uptake, and caused copper deficiency or overload in the deadly Menkes disease and Wilson disease, respectively.[2–4] In many biological fluids copper is present in low molecular weight (LMW) complexes with peptides and amino acids, which take part in copper trafficking in the organism.[1,5–8] Specifically, LMW copper(II) complexes chelated with two amino acids [Cu(aa)$_2$] have been isolated

from normal human blood serum and reported to be part of an exchangeable serum pool for copper.[6,7] It was shown that a majority of these physiological Cu(aa)$_2$ compounds were Cu^{II} complexes with L-histidine (L-His) in the form of electrically neutral bis(L-histidinato)copper(II) [Cu(L-His)$_2$], and ternary complexes favorably with L-asparagine (L-Asn), L-threonine (L-Thr), and L-glutamine (L-Gln).[1,6–8] These amino acids have three functional groups as potential binding sites for metal ions: the α-amino and carboxylate groups, and a side-chain group specific for each amino acid – imidazole in L-His, hydroxyl —OH in L-Thr, and amido —CONH$_2$ in L-Asn and L-Gln. Therapies based on the copper(II)-L-His supplementation are operative in the treatment of Menkes disease.[8–11] Besides, the copper chelation therapy for treatment of neurodegenerative disorders (such as Parkinson, Alzheimer, Creutzfeldt Jakob) and several types of cancers has been under development in the last decades.[4,12,13]

LMW copper(II) coordination compounds typically comprise four nearby donor atoms arranged approximately in a plane around the metal ion, with the possibility of one or two more distant axial donor atoms due to the Jahn-Teller effect.[14–16] When a potentially tridentate amino acid forms a chelate with copper(II), there are many possibilities of both axial and planar bonds. Conversely to the solid-state structural characterization, which generally results with an exact and unique structure, the determination of structure(s) in solutions (which may not be identical to the solid state one) is complicated by the possibilities of different complexing species, coordination numbers and geometries dependent on the pH, temperature, solvent composition, a ratio of the metal and ligand. Thus, the

[a] Prof. M. Ramek, Dr. M. Marković, I. Mutapčić, Prof. A.-M. Kelterer
Institute of Physical and Theoretical Chemistry
Graz University of Technology
Stremayrgasse 9, A-8010 Graz, Austria
[b] J. Pejić, Dr. J. Sabolović
Institute for Medical Research and Occupational Health
Ksaverska cesta 2, HR-10000 Zagreb, Croatia
Homepage: https://www.imi.hr/en/djelatnik/sabolovic-jasmina-2/
E-mail: jasmina.sabolovic@imi.hr

determination of an exact structure of the LMW copper(II) complexes in solutions is far from being an easy task neither experimentally nor computationally.

During the last years we have performed quantum-chemical conformational analyses of Cu(L-His)$_2$,[17] bis(L-threoninato)copper(II) [Cu(L-Thr)$_2$],[18] and (L-histidinato)(L-threoninato)copper(II) [Cu(L-His)(L-Thr)][19] aimed at elucidating the structural properties of physiological Cu(aa)$_2$ species in solutions. As a continuation of these analyses, this paper investigates the structural properties, energy landscapes, and structure–magnetic property relation of physiological bis(L-asparaginato)copper(II) [Cu(L-Asn)$_2$] and (L-histidinato)(L-asparaginato)copper(II) [Cu(L-His)(L-Asn)] in different surroundings using the density functional theory (DFT) method with the B3LYP[20–23] functional.

The LMW copper(II) complexes with L-His and L-Asn may also be considered model systems for studying the noncovalent interactions between the amino-acid side chains around copper in proteins. L-His binds with an unprotonated imino nitrogen atom to transition metal ions in many active sites of metalloproteins. In the type 1 electron-transfer copper proteins, like plastocyanin, it was found experimentally[24] and computationally[25,26] that the formation of hydrogen bonds between the L-Asn side chain and L-serine (L-Ser), and between the L-Asn main chain NH and L-cysteine as well, is crucial for maintaining the active site geometry and functionality. These L-Asn and L-Ser are adjacent to the L-His and L-cysteine, respectively, which are bound to copper in the active site. White et al. studied the metal complex equilibria in xylem fluids and suggested that the major portion of Cu was bound to L-Asn and L-His.[27] Intracellular L-Asn levels are suggested to regulate amino-acid uptake in cells, especially of L-Ser, L-arginine and L-His.[28] Besides, L-Asn is considered an important regulator of cancer cell amino acid homeostasis, anabolic metabolism and proliferation.[28,29]

The solid-state copper(II)-L-Asn complexes were characterized by the IR spectra [Cu(L-Asn)$_2$,[30,31] Cu(L-His)(L-Asn)[32]], a Raman spectrum of Cu(L-Asn)$_2$,[30] the electron paramagnetic resonance (EPR) spectra of Cu(L-Asn)$_2$[33–35] and by the X-ray single crystal structural analysis.[36,37] Cu(L-Asn)$_2$ crystallized as an anhydrous *trans* compound.[36] The X-ray crystal and molecular structures of an anhydrous Cu(L-His)(L-Asn) complex and an aqua trihydrate [Cu(L-His)(L-Asn)(H$_2$O)·3H$_2$O] modification were determined.[37]

In aqueous solutions, the potentiometric[32,38–41] calorimetric,[39–42] polarographic,[43] and EPR[44–47] measurements of copper(II)-asparaginato systems suggested that at pH < 9 the coordination sites of L-Asn to Cu(II) are the same as those of glycine (Gly) (namely, the amino and carboxylate groups), and that the side-chain amido group is not involved. In the pH range 10–12, the spectroscopic results (optical rotary dispersion,[48,49] electronic absorption spectra,[47,49] NMR,[50] EPR[47]) detected an axially bound L-Asn amido group, its deprotonation and the axial bond strengthening. If both amido groups in the bis-complex are deprotonated, the second one is bound equatorially.[47]

The stability constants (log β) of both, Cu(L-Asn)$_2$ and Cu(L-His)(L-Asn), were determined in aqueous solutions at different ionic strengths and temperatures using potentiometric titrations and calorimetry. For Cu(L-Asn)$_2$, log β is 14.45 (0.1 M KNO$_3$, 25°C),[38] 14.142 (0.15 M NaClO$_4$, 37°C),[51] and 16.042 (3.0 M NaClO$_4$, 25°C).[39] The corresponding Cu(L-His)(L-Asn) log β values were 17.03,[32] 16.810,[51] and 18.597.[40] Thus, the stability constant of the ternary Cu(L-His)(L-Asn) was larger than that of the parent Cu(L-Asn)$_2$. Baxter and Williams obtained a greater Gibbs free energy change (−ΔG) for the formation of the ternary complex from an increased entropy change ($T\Delta S$) and a lower than expected enthalpy change (−ΔH).[40] They hypothesized that the increased $T\Delta S$ might be due to more water molecules released from the copper solvation sphere upon forming the ternary than the binary complex, which in turn caused the decrease of −ΔH because more aquation bonds were broken.[40]

The stability constants were used to compute the amounts of the species present at blood plasma pH values (7.3–7.4) under the experimental conditions applied. For the Cu^{II}/L-His/L-Asn system (0.1 M KNO$_3$, 25°C), the total copper was distributed in 72% Cu(L-His)(L-Asn), 14% Cu(L-Asn)$_2$, and 13% Cu(L-His)$_2$.[32] A similar result was obtained for the copper(II)-L-His systems with either L-Thr, L-Gln, or L-Ser, that the ternary species predominated at pH > 6.5, and that the protonated species were negligible in solutions of pH > 3.45.[32] Baxter and Williams computed the species distribution at the L-His, L-Asn, and Cu^{II} blood plasma concentrations by using the stability constants determined in 3.0 M NaClO$_4$ solution at 25°C, and obtained Cu(L-His)$_2$ and Cu(L-His)(L-Asn) as the major species with 55% and 30% total copper, respectively.[40] Brumen et al. computed the distribution of Cu^{II} in the ultrafiltrable fraction of normal blood plasma by using the stability constants determined from potentiometric titrations in 0.15 M NaClO$_4$ (blood plasma ionic strength) at 37°C.[51] The largest percentage of ultrafiltrable copper was calculated to be in Cu(L-His)$_2$ and the ternary L-His complexes with L-Gln and L-Thr (15.5%, 19.2%, and 14.7%, respectively) whereas 4.2% of total Cu^{II} was predicted to be in Cu(L-His)(L-Asn). Common to these studies is that the electrically neutral species predominated. Such species would be favored in the transport of Cu^{II} in hydrophobic environments such as biological membranes.

The overviewed experimental studies of the title Cu(aa)$_2$ complexes were intensive during the 1970s through the 1980s. However, they did not determine the exact structures of the complexes in solutions. In this study we resolved that missing piece of information, and reinterpreted some of the experimental outcomes accordingly. The aim of the study is to determine the exact structures and gain new information about the environmental effects on the structural properties of physiologically important Cu(aa)$_2$ in aqueous solution, as part of their physicochemical characterization for potential use in medicine. Emphasis is given to relate the apical coordination to the Cu^{II} with available experimental evidences on the title complexes in solutions. In aqueous solutions at physiological pH, the coordination mode of Cu(L-Asn)$_2$ was suggested to be glycine-like because the stability constants were very similar to those of the Cu(aa)$_2$ complexes that could have only the amino nitrogen (N$_{am}$) and carboxylato oxygen (O) atoms coordinated to the Cu^{II} with formation of a five-member chelate ring.[38,39,41,44,45] How-

ever, the question whether the amido group was also coordinated to the Cu^{II} (and formed a six- or seven-member chelate ring with either the N$_{am}$ or O atom) could not be definitely answered from the available experimental results. To resolve the dilemma, this paper examines the relative stability of conformers in all possible in-plane binding modes of Cu(L-Asn)$_2$. Systematic conformational analyses in the gas phase and in implicitly modeled aqueous surroundings using a polarizable continuum model (PCM)[52,53] were performed for Cu(L-Asn)$_2$ and Cu(L-His)(L-Asn) to locate the low-energy conformers, and rationalize the effect of noncovalent interactions on the coordination modes and overall geometries of the complexes. Coordination of explicit water molecules to the apical position of selected low-energy conformation was included in the study. The predicted lower-energy aqueous structures are used for DFT calculations of the g-factor and hyperfine coupling constant (HFCC) for a quantitative comparison to experimental EPR data. The suitability of theoretically modeled aqueous environment to encounter the noncovalent interactions was examined by comparing the experimental X-ray molecular structures with the ones calculated in the gas phase and aqueous solution. The computational outcomes were compared for the title complexes with previously obtained ones for physiological Cu(L-His)$_2$,[17] Cu(L-Thr)$_2$,[18] and Cu(L-His)(L-Thr).[19]

2. Results and Discussion

2.1. Defining In-Plane Binding Modes

Cu(L-Asn)$_2$. The trifunctional nature of L-Asn leads to a flexidentate coordination. In addition to the amino nitrogen (N$_{am}$), and carboxylate oxygen (O) donor atoms, the −CONH$_2$ group contains two different donor atoms and therefore may be coordinated by the amidic nitrogen (N$_{ad}$) or oxygen (O$_{ad}$) atom. For the nomenclature of various in-plane binding modes of L-Asn to Cu(II), we term −C$^\beta$H$_2$−C$_{ad}$O$_{ad}$−N$_{ad}$H$_2$ as "side chain" and H$_2$N$_{am}$−C$^\alpha$H−C$_c$OO as "main chain" (see Scheme 1 for atom labeling). In the mode names (Scheme 2), we denote the in-plane binding of N$_{ad}$ and O$_{ad}$ from the side chain by lower case letters, and the binding of N$_{am}$ and O from the main chain by upper case letters. Hence, "Oo" will indicate the mode in which O and O$_{ad}$ bind to copper, and "On" will indicate that O and N$_{ad}$ bind to copper. "NO" will stand for the glycinato mode, in which the main chain atoms, N$_{am}$ and O, bind to Cu. The "no" mode,
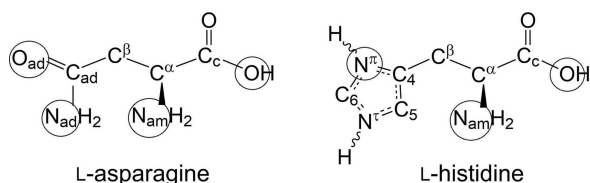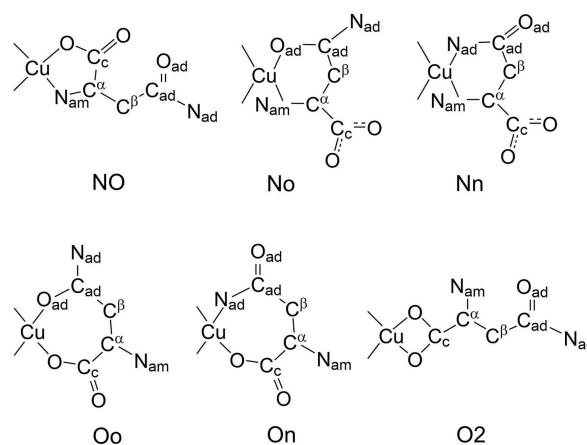
Scheme 2. Defining the coordination mode names in Cu(L-Asn)$_2$ (the chelate atoms are given in parentheses): NO (N$_{am}$ and O), No (N$_{am}$ and O$_{ad}$), Nn (N$_{am}$ and N$_{ad}$), Oo (O and O$_{ad}$), On (O and N$_{ad}$), O2 (two carboxylate O atoms).
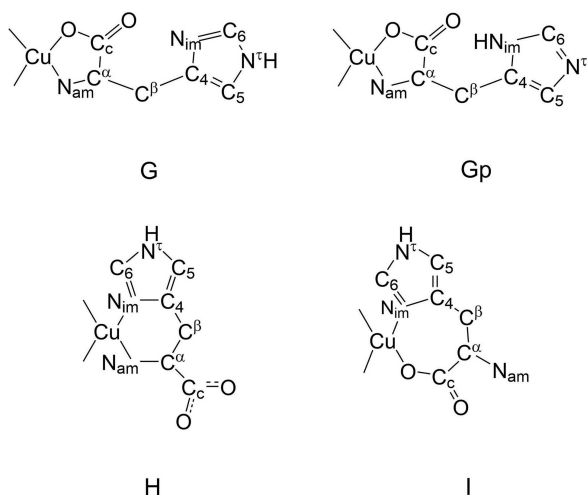
with N$_{ad}$ and O$_{ad}$ binding to the central Cu^{II}, was considered to be sterically improbable.

By applying this notation to the binding of two L-Asn in the bis-complex, we can distinguish 15 unique in-plane coordination-mode combinations: NONO, NONo, NONn, NOOn, NOOo, NnOn, NnNo, NnOo, NoOo, OnOo, NoOn, NnNn, NoNo, OoOo and OnOn.

In all of these modes, the two amino acids can combine in an equatorial plane relative to each other in a *cis* or *trans* configuration, which we indicated by a leading "c" or "t". While *cis* and *trans* configurations are easy to define for the NONO mode, this becomes a challenge for the mixed main- and side-chain binding modes. To keep the definition simple in these cases, the main chain atoms are given precedence. It should be noted that this rule can sometimes result in e.g. a *trans* structure, in which two oxygen and two nitrogen atoms will be next to each other (like in tNoOn) but the two main group atoms bound to Cu are opposite of one another, hence the classification *trans*.

Cu(L-His)(L-Asn). L-His has three possible donor atoms: amino group N$_{am}$, imidazole N$^\pi$ (N$_{im}$), and carboxylate O, which can form three different in-plane binding modes as described in details elsewhere:[17,54] G, H, and I for glycine-like (N$_{am}$ and O bind to the copper), histamine-like (N$_{am}$ and N$_{im}$ are the donor atoms), and imidazole–propionic acid (impa)-like mode (O and N$_{im}$ are the chelating atoms), respectively. These modes are illustrated in Scheme 3.

In the physiological pH range, the L-His imidazole ring is neutral, i.e. only one of the two nitrogen atoms (N$^\pi$ or N$^\tau$) carries a hydrogen atom (Scheme 1). The thermodynamic parameters (stepwise enthalpies and entropies of formation) measured for the L-hystidyl-copper(II)-proton system in aqueous solution (3.0 M NaClO$_4$, 25 °C) suggested that the complexes existing in aqueous solution were of only one tautomer, the N$^\tau$-protonated one with N$^\pi$ as the potential chelating atom.[55] In line with that, the study of Cu(L-His)(L-Thr) showed that generally, the glycinato-mode conformers with protonated N$^\tau$

Scheme 1. The atom labeling in L-asparagine (L-Asn) and L-histidine (L-His) used in this paper. Either N$^\tau$ or N$^\pi$ can be protonated. The chelating atoms discussed in this paper are denoted by the circles.

Scheme 3. The coordination mode names of L-His in Cu(L-His)(L-Asn) (hydrogen atoms are omitted for clarity) as follows: glycine-like mode with N^τ protonated (G), glycine-like mode with N^π (N_{im}) protonated (Gp), histamine-like mode (H), and impa-like mode (I).

Table 1. Number of Cu(L-Asn)$_2$ conformers as follows: in 15 *trans* ("t") and 15 *cis* ("c") in-plane bidentate coordination modes, with tetrahedral ("Td") copper(II) coordination geometry, in O2 modes, and with monodentate binding ("mono-bi") of one or two L-Asn to the copper(II) in the gas phase and implicitly modeled aqueous solution.

Mode	Gas phase	Aqueous solution	Mode	Gas phase	Aqueous solution
tNONO	31	74	cNONO	17	66
tNOOo	36	54	cNOOo	35	53
tNONo	15	29	cNONo	26	32
tNOOn	53	62	cNOOn	30	74
tNONn	27	54	cNONn	26	47
tOoOo	15	13	cOoOo	11	11
tNoNo	8	4	cNoNo	6	9
tNoOo	12	9	cNoOo	13	19
tNnOo	15	15	cNnOo	15	15
tOnOo	20	26	cOnOo	13	27
tOnOn	16	19	cOnOn	4	16
tNnNo	6	10	cNnNo	6	13
tNoOn	9	28	cNoOn	20	19
tNnOn	17	29	cNnOn	8	20
tNnNn	1	11	cNnNn	0	13
O2NO	38	2	O2No	16	0
O2Oo	19	0	O2On	28	10
O2O2	6	0	O2Nn	18	0
Td	103	1	mono-bi	21	20

have a lower energy, but several conformers with protonated N^π are in a comparable energy range.[19] Hence, the glycinato-mode initial structures were prepared in both variants, and the N^π-protonated ones are labelled as "Gp" (Scheme 3).

Consistently with the results of conformational analyses of Cu(L-Asn)$_2$ (see 2.3), we decided to restrict the systematic conformational search of Cu(L-His)(L-Asn) to L-Asn in the glycinato mode only. Due to this decision, "N" is used as the symbol for L-Asn in the ternary complex conformers. Hence, we term the Cu(L-His)(L-Asn) conformers in possible L-His (G, Gp, H, and I) and L-Asn (N) coordination combinations as GN, GNp, HN and IN, respectively. Initial structures were generated with an approximate square planar arrangement around the copper atom with the N_{am} atoms of the GN, GNp, and HN modes, and the carboxylato O atoms of the IN mode in the *cis*- and the *trans*-configuration (indicated by a leading "c" or "t" in the conformer names).

For both systems under scrutiny, geometry optimizations were performed in the gas phase as well as in an implicitly modeled aqueous solution. The latter was carried out using PCM, the details of which are given in the Computational Methods section at the end of the Article. For selected low-energy PCM aqueous geometries with different binding modes, the effect of an apically coordinated water molecule was investigated.

In the Supporting Information, the gas-phase names, relative electronic energies (ΔV_{vacuum}) and characteristic torsion angles of all obtained gas-phase conformers are collected in tables as follows: Tables S1–S38 for Cu(L-Asn)$_2$, and Tables S73–S81 for Cu(L-His)(L-Asn). For the minimum structures in aqueous medium, the same corresponding data and relative electronic energies (ΔV_{water}) and Gibbs free energies (ΔG_{water}) are provided in Tables S39–S72 for Cu(L-Asn)$_2$, and Tables S82–S89 for Cu(L-His)(L-Asn). Figures S1–S5 and Figures S6–S7 present the illustrations of up to five gas-phase and aqueous minima, respectively, with lowest electronic energies in each of the coordination modes of Cu(L-Asn)$_2$ and Cu(L-His)(L-Asn). The conformers are sorted and named by the mode and the electronic energy values, from lowest to largest values, with "1" in the name for the lowest-energy minimum of a specific mode. The PCM aqueous conformers are distinguished from the gas-phase ones by an additional letter "w" in front of the number in the names. Selected lower-energy aqueous conformers of the title complexes interacting with one and two explicit water molecules are further differentiated by additional letter "a" and "b", respectively, in the names (Figure S8).

Cu(L-Asn)$_2$. The conformers with the lowest overall electronic energy values are tNONO1 in the gas phase, and

2.2. Minimum Structures by Geometry Optimizations

The geometry optimizations for Cu(L-Asn)$_2$ resulted in a total of 760 conformers in the gas phase and 904 conformers in aqueous solution (Table 1). The geometry optimizations of Cu(L-His)(L-Asn) yielded a total of 475 conformers in the gas phase and 661 conformers in aqueous solution (Table 2).

Table 2. Number of B3LYP gas-phase and aqueous PCM *cis*- and *trans*-Cu(L-His)(L-Asn) minima in the corresponding coordination modes.

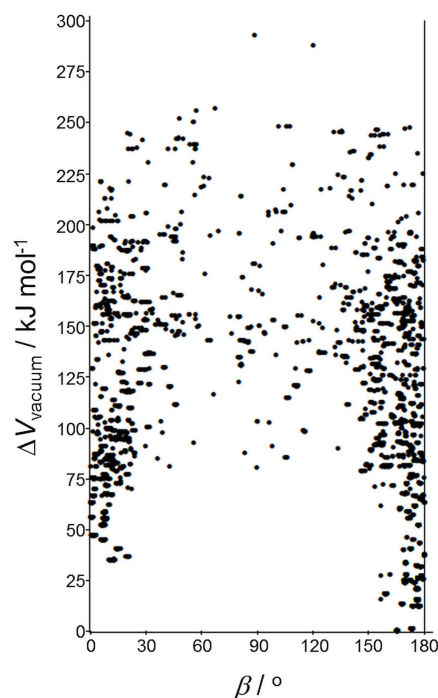| Mode	Gas phase		Aqueous solution	
	trans	*cis*	*trans*	*cis*
GN	69	63	127	122
GNp	112	111	132	121
HN	5	16	22	25
IN	59	40	62	50
Total	245	230	343	318
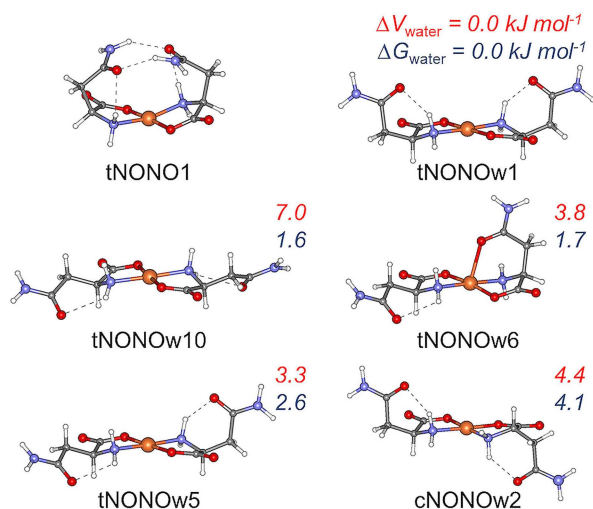
Figure 1. The most stable Cu(L-Asn)$_2$ structures: gas-phase conformer tNONO1, and five aqueous conformers with lowest Gibbs free energies, G_{water}. The relative electronic (ΔV_{water}) and ΔG_{water} energies of the aqueous conformers are printed in italic. Hydrogen bonds are depicted by dashed lines.

Figure 2. Gas-phase electronic energy dependence on the angle β between the normal vectors to the planes defined by $<$Cu, X, Y$>$ and $<$Cu, X', Y'$>$, where X and Y are donor atoms of one amino acid, and X' and Y' are donor atoms of another amino acid in Cu(L-Asn)$_2$. The β values of 0° and 180° correspond to the cis and trans, respectively, square-planar copper environment, and β values around 90° indicate a tetrahedral arrangement.

tNONOw1 in aqueous solution (Figure 1). The energies of these two conformers (Tables S2 and S39, respectively) are used as the reference values in the respective environments. Although the starting conformations were prepared for all of the 30 in-plane binding modes, some of the geometry optimizations yielded yet another new binding motif; namely, one in which both oxygen atoms from the same carboxylato group bind to Cu^{II}. In the nomenclature sketched above, this would be an "OO" mode, which we called "O2" (Scheme 2) as a more easily recognizable symbol. As a matter of fact, the combination of O2 with all in-plane binding modes was found (Table 1). It should be stressed that we did not specifically look for these O2 conformers, but those, that we obtained by geometry optimization, we did define and list in the Supporting Information (Tables S31–S36 and Tables S69–S70; Figures S2 and S4). Interestingly, while there are 125 such conformers obtained in the gas phase, only 12 are stable in aqueous solution (Table 1). Additionally, some optimizations resulted in at least one L-Asn bound to copper with only one hetero atom, i.e., its binding was no longer bidentate (Table 1). Those structures are listed in the Supporting Information Tables S38 and S72.

Although all minima are listed in the Supporting Information, those with the O2 mode and the coordination number less than 4 were not analyzed further because (i) such structures were not outlined by experimental studies overviewed in the Introduction as physiologically important species, and (ii) the relative energies of their most stable conformers are rather high [≈ 51–59 kJ mol^{-1} for cO2NO1 (Figure S2) and cO2Now1 (Figure S4); 78.6 and 148.8 kJ mol^{-1} for the three-coordinate Cu(L-Asn)$_2$ NOO1 and OoOw1 conformers, respectively].

Another feature of the optimized structures is the fact that a distorted-planar arrangement around copper is, for some binding modes, not the only one obtained. Figure 2 depicts the relative gas-phase electronic energy as a function of the angle β

between two half-planes of copper and its donor atoms in each L-Asn ligand. The planar copper(II) coordination geometry is an electronically favored structure for Cu(aa)$_2$ complexes, and an intramolecular steric hindrance can be alleviated either by distortion of the copper(II) coordination polyhedron and/or by changing the geometry of the chelate rings.[56] Figure 2 shows that the approximate square-planar arrangement, which is predominant at low-energy structures, becomes more and more distorted until, for high-energy conformers, a tetrahedral arrangement is formed. To make these easily identifiable, we changed the label "c" to "z" and "t" to "x" (Table S37) if the β angle between the two planes of copper and the respective amino acids was in the range of 45° to 135° (Figure 2). Figure S3 illustrates several such minima.

Cu(L-His)(L-Asn). The gas-phase and aqueous conformers with the lowest overall electronic energy, tGN1 and tGNw1, are illustrated in Figure 3. tGNw1 is also the conformer with the overall lowest Gibbs free energy in aqueous solutions (Table S82). The energies of these two conformers were used as reference values in the respective environments.

2.3. Conformational Analyses

The DFT/B3LYP conformational analyses of Cu(L-Asn)$_2$ and Cu(L-His)(L-Asn) performed in the gas phase and in implicitly modeled aqueous solution were used to study the influence of
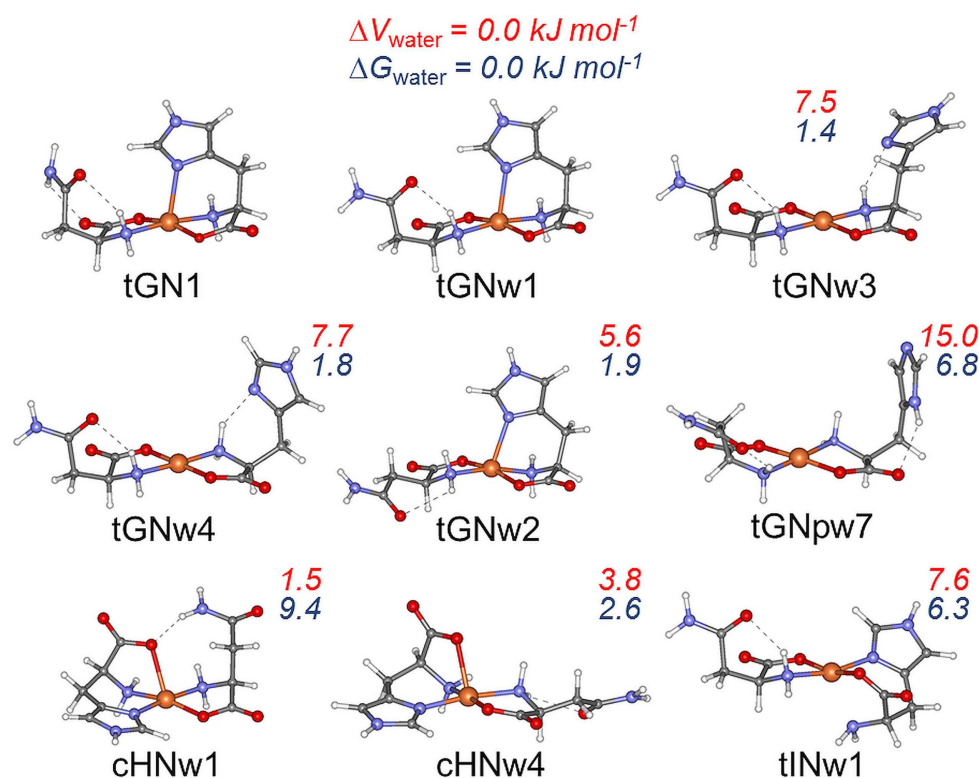
Figure 3. The most stable gas-phase conformer tGN1, and aqueous Cu(L-His)(L-Asn) structures: four conformers with the lowest Gibbs free energies (the tGN conformers), and the conformers with the lowest electronic (V_{water}) and/or Gibbs free energies (G_{water}) in each group of the GNp, IN, and HN conformers. Relative ΔV_{water} (red) and ΔG_{water} (blue) values are given in italic. Hydrogen bonds are shown with dashed lines.

intermolecular interactions between the complexes and water medium on the stability of coordination modes and overall geometries. The energy landscapes of aqueous (Figures 4 − 6) and isolated (Figures 5, S9 and S10) systems were compared. It should be stressed that a complete conformational landscape of an isolated complex is a prerequisite to rationalize the impact of intermolecular interactions on the geometry of the complex in aqueous solution. For both title complexes, the much larger number of aqueous conformers compared to the gaseous ones (Tables 1 and 2) with a distorted-planar Cu[II] coordination geometry suggests that intermolecular interactions stabilize the conformers which are unstable in the gas phase. Similar results were obtained by the conformational analyses of Cu(L-His)(L-Thr).[19] Additionally, we evaluate the population of conformers in aqueous solution (Tables 3 and 4), analyze apical Cu–donor distances (Table 5), list the means of in-plane Cu–donor bond lengths and valence angles around Cu[II] (Tables S90–S92), as well as the number of intra- and inter-ligand hydrogen bonds (Tables S93–S95) in the title complexes.

Energy Landscapes of Cu(L-Asn)₂. The energy landscapes of isolated and aqueous Cu(L-Asn)₂ are shown in Figures S9 and 4, respectively. The most stable aqueous conformer tNONOw1 (Figure 1, Table S39) has the same conformation as gaseous tNONO2 ($\Delta V_{vacuum} = 0.7$ kJ mol^{-1}, Table S2). However, an aqueous counterpart of the most stable gaseous conformer tNONO1, with two intra-ligand and two inter-ligand hydrogen bonds (Figure 1), becomes less stable in aqueous surroundings

Table 3. Statistical weights, w ($\times 100\%$), greater than 0.9%, and relative Gibbs free energies, ΔG_{water} (kJ mol^{-1}), of denoted Cu(L-Asn)₂ conformers in aqueous solution at 298.15 K.[a,b]

| Conformer	ΔG_{water}	w	Conformer	ΔG_{water}	w
tNONOw1	0.0	28.3	cNONOw6	6.9	1.8
tNONOw10	1.6	14.9	cNONOw1	7.0	1.7
tNONOw6	1.7	14.3	tNONOw4	7.0	1.7
tNONOw5	2.6	9.9	cNONOw10	7.8	1.2
cNONOw2	4.1	5.4	tNONOw13	7.8	1.2
tNONOw2	4.8	4.1	tNONOw21	8.0	1.1
tNONOw3	5.1	3.6	tNONOw7	8.3	1.0
tNONOw8	5.2	3.5	cNONOw5	8.4	1.0

[a] The w values were calculated using Equation (1) (see Computational Methods) by accounting 230 conformers in the NONO and NONo modes. $G_{water,min}$ in Equation (1) was equal to the Gibbs free energy of the tNONOw1 conformer (Table S39). [b] The conformers are defined in Tables S39–S42.

(tNONOw34, $\Delta V_{water} = 17.7$ kJ mol^{-1}; $\Delta G_{water} = 31.5$ kJ mol^{-1}, Table S39). The single aqueous tetrahedral conformer (Figure 4, Table S71) compared to the 103 in the gas phase (Figure S9, Table S37) suggests that the interactions between the complex and the water solvent can cause the intramolecular hydrogen bonds to break with a subsequent relaxation to distorted planar structures of lower energy.

The energy landscapes show that the most stable conformers are in the tNONO mode, distinctively in the gas phase (Figure S9), while in aqueous solution, both tNONO and cNONO conformers can have comparable energies (Figure 4). This is in
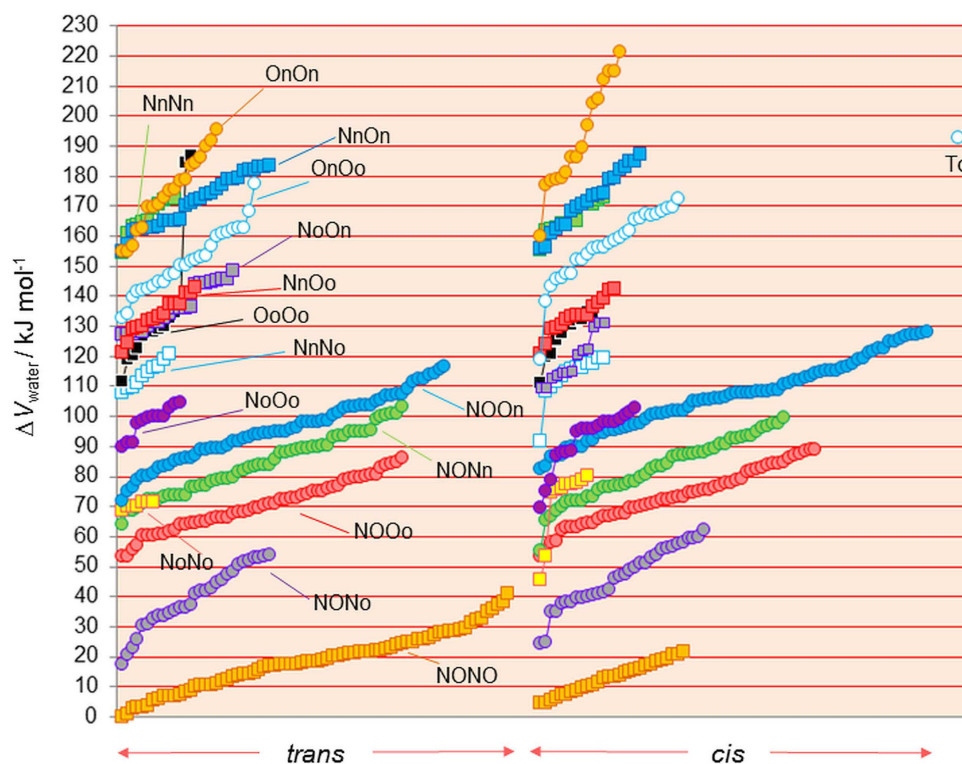
Figure 4. Relative B3LYP electronic energies, ΔV_{water}, of the *trans*- and *cis*-Cu(L-Asn)$_2$ conformers in the denoted coordination modes in simulated aqueous environment. The electronic energy of tNONOw1 is the reference value (Table S39). "Td" denotes the tetrahedrally distorted conformer.
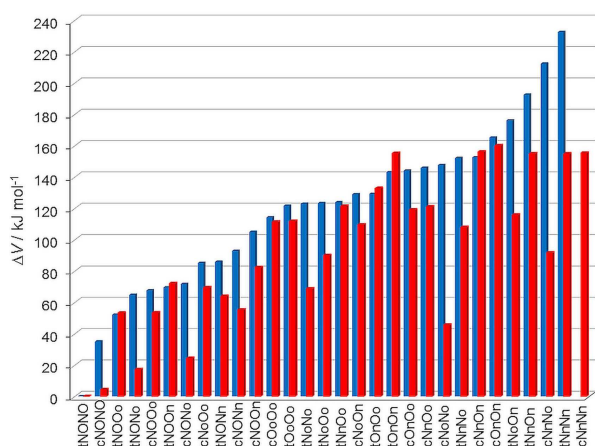
Figure 5. Comparison of relative electronic energies (ΔV) for the lowest-energy Cu(L-Asn)$_2$ conformers in each of the in-plane modes in the gas phase (blue, left column) and PCM-estimated aqueous solution (red, right column).

Table 4. Statistical weights, w ($\times 100\%$), greater than 0.96%, and relative Gibbs free energies, ΔG_{water} (kJ mol^{-1}), of the denoted Cu(L-His)(L-Asn) conformers in aqueous solution at 298.15 K, and the weighted ΔG_{water} averages calculated separately for the conformers in each coordination mode.[a,b]

Conformer	ΔG_{water}	w	conformer	ΔG_{water}	w
tGNw1	0.0	12.6	tGNw35	4.6	2.0
tGNw3	1.4	7.2	cHNw3	4.6	2.0
tGNw4	1.8	6.1	cGNw1	4.8	1.8
tGNw2	1.9	5.9	tHNw1	4.9	1.8
tGNw13	2.3	5.0	tHNw3	5.0	1.7
cHNw4	2.6	4.4	tGNw14	5.1	1.6
cHNw2	3.1	3.6	tGNw34	5.5	1.4
cGNw3	3.2	3.5	tGNw23	6.0	1.1
cGNw2	3.3	3.3	cGNw9	6.2	1.0
tGNw12	3.8	2.7	tINw1	6.3	1.0
tGNw18	3.9	2.6	tGNw17	6.3	1.0
cGNw7	4.4	2.1	tINw3	6.4	1.0

$<\Delta G_{water}>$/kJ mol^{-1}

tGN	cGN	tGNp	cGNp	tHN	cHN	tIN
3.3	5.7	9.9	14.2	6.0	4.0	7.1

[a] The w and $<\Delta G_{water}>$ values were calculated for 475 conformers using Equations (1) and (2), respectively (see Computational Methods). The $G_{water,min}$ in Equation (1) was equal to the Gibbs free energy of the tGNw1 conformer (Table S82). [b] The conformers are defined in Tables S82–S89.

accord with the EPR spectra measured for Cu(L-Asn)$_2$, which indicated that both *cis* and *trans* isomers with the CuN$_2$O$_2$ chromophore were in equilibrium in aqueous solution.[44,45] Specifically, ΔV between the lowest-energy tNONO and cNONO conformers dropped from 35.0 kJ mol^{-1} (ΔV_{vacuum}) to 4.4 kJ mol^{-1} (ΔV_{water}). This seems to be a common characteristic for *trans* and *cis* glycinato-mode Cu(aa)$_2$ conformers, that they have similar stability in aqueous solution at room

temperature[18,19,57–61] while the *trans* conformers are more stable as isolated compounds.[17–19,58–63]

Comparison of relative electronic energies (ΔV) for the lowest-energy conformers in each of the in-plane modes in the gas phase and PCM-estimated aqueous solution (Figure 5) shows that ΔV are much lower by PCM than in the gas phase

Table 5. Means, standard deviations (in parentheses), and number (*N*) of the B3LYP Cu–donor apical bond distances (< 3.0 Å) in *trans* and *cis* conformers of Cu(L-Asn)$_2$ (the NONO and NONo modes) and Cu(L-His)(L-Asn) (the GN, GNp, HN, IN modes) in the gas phase and PCM-calculated aqueous solution.

	Cu–N$_{im}$	N[a]	Cu–N$_{am}$	N[a]	Cu–O	N[a]	Cu–N$_{ad}$	N	Cu–O$_{ad}$	N[a]
Gas phase										
tNONO							2.67(7)	5	2.5(1)	6
cNONO							2.7(1)	3	2.92(5)	3
Aqueous solution										
tNONO							2.87(6)	9	2.38(3)	11 [3]
cNONO							2.91(4)	8	2.38(4)	10 [2]
Gas phase										
tNONo							2.64(5)	2	2.42(1)	3
cNONo					2.178	1	2.624	1	2.37(6)	5
Aqueous solution										
tNONo					2.25(3)	5	2.75(3)	3	2.38(8)	3
cNONo					2.24(4)	5	2.8(1)	3	2.332(4)	2
Gas phase										
tGN	2.38(4)	10					2.63(2)	3	2.48(3)	5
cGN	2.35(5)	10							2.88(9)	3
tGNp	2.941	1					2.67(6)	7	2.4(1)	11
cGNp	2.98(2)	2					2.62(4)	10	2.7(2)	9
tHN										
cHN					2.24(6)	2			2.36(6)	3
tIN			2.33(4)	9			2.62(6)	4	2.46(5)	4
cIN			2.29(1)	6			2.7(2)	4	2.612	1
Aqueous solution										
tGN	2.336(8)	8 [5]					2.84(5)	3	2.40(7)	12 [6]
cGN	2.33(2)	10 [3]							2.38(6)	14 [1]
tGNp							2.9(1)	2	2.38(3)	12
cGNp							2.91(5)	3	2.360(5)	12
tHN					2.264(9)	10 [3]			2.4(1)	3
cHN					2.29(2)	11 [6]			2.356(7)	2
tIN			2.29(1)	10 [2]			2.79(7)	3	2.4(1)	6
cIN			2.271(7)	10			2.8(1)	3	2.37(2)	4

[a] The numbers in square brackets represent the occurrence of apical coordination among 21 Cu(L-Asn)$_2$ and 57 Cu(L-His)(L-Asn) conformers with $\Delta G_{water} \leq 10.0$ kJ mol^{-1}.

for the conformers in the No and Nn modes. For the On and Oo conformers with seven-member chelate rings, similar ΔV values were obtained in both environments (Figure 5). Although the NONo conformers are highly unfavorable in the gas phase (Figures S9 and 5), the ΔV values of the most stable aqueous NONo conformers were significantly lowered (by 47.5 kJ mol^{-1}) and became comparable to the energies of the NONO conformers (Figures 4 and 5). The energy drop suggests that the No conformers can form favorable intermolecular interactions with the solvent. In turn, the intermolecular interactions stabilize the lowest-energy NONo aqueous conformers with apically coordinated carboxylate O atom(s) (Figure S11; Table 5). Such an axial coordination was achieved in only one NONo conformer in the gas phase (Table 5), for cNONo1 (Figure S1), in which an inter-ligand C$^{\beta}$–H···O interaction is formed. A similar result was obtained by the B3LYP calculations of isolated and aqueous Cu(L-His)$_2$,[17,54] and Cu(L-His)(L-Thr) conformers,[19] that the axial coordination of carboxylato O atom(s) can be stabilized only by intramolecular and/or intermolecular non-covalent interactions.

Hence, in the PCM energy landscape (Figure 4), only NONO and NONo conformers are present within a relatively large ΔV_{water} range from 0.0 to 45.0 kJ mol^{-1}. Thus, it may be assumed that the conformers solely in these modes are in equilibrium in aqueous solution at room temperature. An evaluation of their statistical weights using Equation (1) (see Computational Meth-

ods) indicates that 16 NONO conformers (Table 3) with the lowest G_{water} cover the population of 94.7%. The evaluation gave very small chances of 0.01% for the population of the most stable NONo conformers tNONow1 and tNONow2 (Figure S11). The dominance of the NONO conformers supports the supposition based on experimental evidences[38,39,41] that the prevailing Cu(L-Asn)$_2$ species in aqueous solutions at physiological pH is in glycinato mode.

Energy Landscapes of Cu(L-His)(L-Asn). The energy landscapes of the isolated and aqueous ternary complex are presented in Figures S10 and 6, respectively. Again, the glycinato-type conformers are the most stable in the gas phase (Figure S10). Generally, *trans* conformers in all modes except HN were more stable than the *cis* ones in the gas phase. In aqueous solution, not only the cGN but also the cHN and tHN conformers can have comparable stability with the tGN ones (Figure 6).

The DFT/B3LYP conformational analysis of Cu(L-His)(L-Asn) in aqueous solution resulted in a considerable number of lower-energy conformers (Figure 7) as 57 conformers in different coordination modes have $\Delta G_{water} \leq 10.0$ kJ mol^{-1} (28 tGN, 11 cGN, 3 tHN, 6 cHN, 3 tIN, 6 tGNp). By assuming that the aqueous conformers are in equilibrium at 298.15 K, the statistical weights, *w* (Equation (1) in the Computational Methods section), for each of the PCM-calculated Cu(L-His)(L-Asn) conformers were computed to evaluate their possible population in
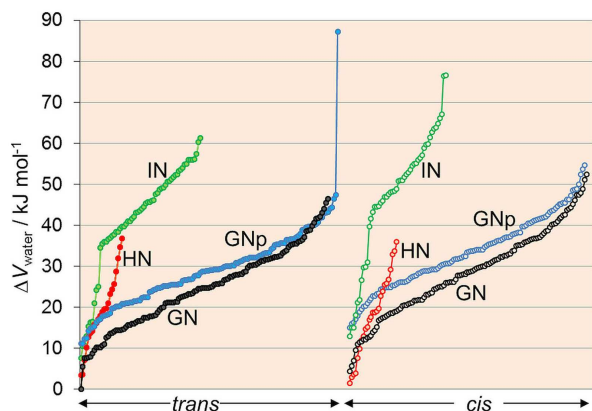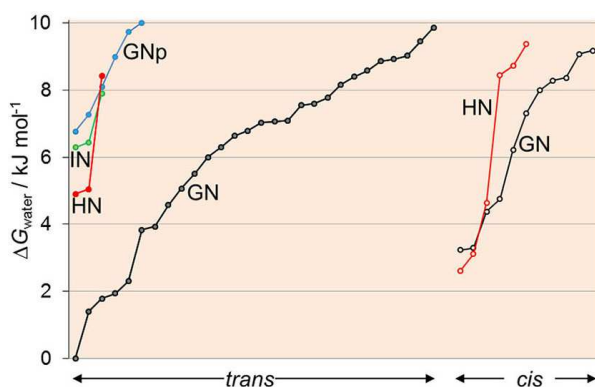
Figure 6. Relative DFT/B3LYP electronic energies, ΔV_{water}, calculated in simulated aqueous environment using PCM for the Cu(L-His)(L-Asn) conformers. The electronic energy of tGNw1 (Figure 3) is the reference value (Table S82).

aqueous solution. The w calculations yielded 24 conformers with the population from 12.6 to 1.0% (Table 4) corresponding to the span of ΔG_{water} from 0.0 to 6.4 kJ mol^{-1}, and covering 75.4% of overall population. 194 conformers had a population from 0.01 to 0.90%, and 443 conformers had no population. A similar computational outcome was obtained for Cu(L-His)(L-Thr).[19]

Among the 24 lower-energy minima (Table 4) are the conformers in the tGN, cHN, cGN, tHN, and tIN modes. The statistical weights of the most stable aqueous conformers in other modes are 0.2% (cINw3), 0.8% (tGNpw7), and 0.2% (cGNpw2). The B3LYP-calculated weighted ΔG_{water} averages (Table 4), evaluated separately for each group of Cu(L-His)(L-Asn) conformers with the same coordination mode, gave the following ranking of thermodynamic stability: tGN $\approx$ cHN > cGN $\approx$ tHN > tIN > tGNp > cIN > cGNp. The same ranking regarding the L-His mode was obtained for the Cu(L-His)(L-Thr) aqueous conformers.[19] The statistical evaluation yielded the $< \Delta G_{water}>$ values for all coordination modes within 15 kJ mol^{-1}

Figure 7. Relative DFT/B3LYP Gibbs free energies, ΔG_{water}, calculated in simulated aqueous environment using PCM, of the lower-energy Cu(L-His)(L-Asn) conformers. The Gibbs free energy of tGNw1 is the reference value (Table S82).

(Table 4), similarly as for the individual ΔG_{water} values (Tables S82–S89).

Hence, the PCM prediction is that the conformers with both amino acids in the glycinato mode in Cu(L-His)(L-Asn) are among the most stable ones in aqueous solution. The same B3LYP outcome was obtained for Cu(L-His)(L-Thr).[19] The predictions are in accord with the experimental absorption and circular dichroism (CD) spectra measured at pH 7–8 for ternary copper(II)-L-His-amino acid complexes.[32] For these complexes, the amino acids with polar side chains, and those that can form only the glycinato-type coordination, exhibited almost invariably the absorption peaks at 610–620 nm in the visible region and positive CD maxima at 620–630 nm, which suggested the same coordinating groups in the Cu^{II} coordination plane.[32]

For Cu(L-His)$_2$, the experimental studies at physiological pH[8,64,65] as well as the computational studies with explicit water molecules[17,54] suggested an equilibrium of a histamine-histamine (HH) and a histamine-glycine (HG) bonding type in a cis-configuration with carboxylato O atom(s) in the axial position (s), while a glycine-glycine mode was considered improbable. Such a fluctuating type of coordination could be maintained by changing a local water molecule environment around Cu(L-His)$_2$, as suggested by the DFT calculations.[17] The tNONow3 minimum of Cu(L-Asn)$_2$ (Figure S11) demonstrates a coordination similar to the HH one; it has two carboxylate O atoms in the axial positions and the No-mode chelate ring which is six-membered like in the cis-HH Cu(L-His)$_2$ aqueous structure. Accordingly, we examined whether a cis-HNo structure of Cu(L-His)(L-Asn) with two six-member chelate rings and two Cu–O apical bonds could be favorable in aqueous solution as it is for cis-HH. Yet, the structure is unstable by B3LYP, since its geometry optimization by using PCM transformed it to the already known six-coordinate tINw6 (Figure S11). Specifically, in the PCM geometry optimization, the O atoms adopted closer equatorial positions, while N$_{am}$ and O$_{ad}$ moved to the farther apical positions. These DFT/B3LYP results additionally support experimental outcomes[32,40,46] on the glycinato in-plane mode of L-Asn in Cu(L-His)(L-Asn).

Apical Cu–donor distances. Baxter and Williams suggested the type of bonding of the L-Thr, L-Asn, and L-His ligands in the ternary copper(II) complexes in aqueous solution, whether it is bi- or tridentate to copper(II) on the basis of thermodynamic parameters (that reflect the bond strengths, ring strains, and configurations) for forming the parent binary and ternary complexes.[40] The values of enthalpy and entropy changes suggested L-Thr to be bidentate, L-His to be tridentate, and L-Asn to be a mixture of bi- and tridentate.[40] Indeed, in the previously predicted set of lower-energy aqueous conformers of Cu(L-His)(L-Thr) (with DFT/B3LYP ΔG_{water} up to 10 kJ mol^{-1}), L-Thr was bidentate and L-His was tridentate (apical Cu–N$_{im}$ and Cu–O bonds were formed).[19] For Cu(L-His)(L-Asn), Baxter and Williams proposed a structure with an H-mode and an axially coordinated O atom for L-His, the glycinato mode for L-Asn, and tentatively gave an advantage to N$_{ad}$ over O$_{ad}$ for a transient coordination in an extended axial position.[40] To examine the supposition, we analyzed the apical Cu-donor coordinative

bonding in Cu(ʟ-Asn)$_2$ and Cu(ʟ-His)(ʟ-Asn) with emphasis on such bonding in lower-energy PCM minima (Table 5).

Generally, in the experimental studies in solutions, the tridentate nature of ʟ-His was exclusively supposed to be in the H mode with an axially placed O in the ternary copper(II) amino acid complexes.[8,32,40,46] Such an ʟ-His coordination was observed in the X-ray crystal structures of Cu(ʟ-His)$_2$,[66] Cu(ʟ-His)(ʟ-Thr),[67] and Cu(ʟ-His)(ʟ-Asn).[37] However, as ʟ-His has three donor groups which may be placed in a unique axial position, two more tridentate binding modes can exist as follows: with apical N$_{im}$ in the GN and GNp conformers, and apical N$_{am}$ in the IN conformers (Table 5). All three axial coordination types were obtained by the B3LYP conformational analysis of aqueous Cu (ʟ-His)$_2$[17] and Cu(ʟ-His)(ʟ-Thr).[19]

For Cu(ʟ-Asn)$_2$ and Cu(ʟ-His)(ʟ-Asn), compared to the corresponding apical Cu–donor bonds in the gas phase, they are much more numerous in aqueous solution when O and O$_{ad}$ are the donors (Table 5). The B3LYP-estimated result is that O$_{ad}$ but not N$_{ad}$ adopted an axial position in the PCM lower-energy minima (Table 5). There are only three cases of the Cu–O apical bonding in the gas phase (Table 5). They are established with the help of inter-residual noncovalent bonding, that is, by a C^β–H···O bonding in the already mentioned cNONo1 as well as in cHN1 (Figure S6), and by an N$_{ad}$–H···O bond in cHN6.

The six-coordinate cases with two longer apical bonds are also seldom, as follows: in cGNw6 (Cu–N$_{im}$ and Cu–O$_{ad}$), tINw6 (Cu–N$_{am}$ and Cu–O$_{ad}$), and tHNw6 (Cu–O and Cu–O$_{ad}$). In the simulated aqueous system, these are the minima whose ΔG_{water} is in the 11.5–14.3 kJ mol^{-1} range, and the population is from 0.12 % to 0.04 %. In the gas phase, only one six-coordinate Cu(ʟ-Asn)$_2$ conformer resulted in cNONO17 with two Cu–N$_{ad}$ longer apical bonds. Two hexa-coordinated conformers were obtained for aqueous Cu(ʟ-Asn)$_2$: tNONow3 (Cu–O and Cu–O$_{ad}$, Figure S11) and cNONOw8 (two Cu–O$_{ad}$; $\Delta G_{water} = 14.3$ kJ mol^{-1}, 0.08 % population).

Hence, all PCM lower-energy minima (within 10 kJ mol^{-1} of ΔG_{water}) with an apical intramolecular interaction are a tridentate-bidentate combination. Among 21 Cu(ʟ-Asn)$_2$ lower-energy minima, five have a Cu–O$_{ad}$ apical interaction (tNONOw2, tNONOw4, tNONOw6, cNONOw1, and cNONOw5; they are listed in Table 3, and comprise 22.8 % of the population). Among 57 Cu(ʟ-His)(ʟ-Asn) lower-energy conformers (Figure 7), 18 have a tridentate ʟ-His, and 7 have a tridentate ʟ-Asn.

Specifically, among the 24 lower-energy Cu(ʟ-His)(ʟ-Asn) conformers (Table 4), 13 have an apical bonding in the ʟ-His ligand (O, N$_{im}$ and N$_{am}$ are placed axially in 5 HN, 7 GN, and 1 tIN conformers, respectively), and 1 has the apical Cu–O$_{ad}$ interaction (tGNw13). These 14 conformers make 43 %, and the other 10 bidentate conformers contribute 30 % to the population in the simulated aqueous system.

In the PCM equilibrium structures of the bidentate-tridentate conformers with one explicit water molecule, tNONOw2_a·H$_2$O and cHNw4_a·H$_2$O (Figure S8), the water molecule (initially at the apical position prior the geometry optimization) positioned equatorially and axially to Cu^{II}, respectively, but did not disturb the intramolecular apical coordination.

Thus, the presented results support the experimental conclusions[32,40,41] on a possible prevalence of tridentate ʟ-His and a combination of bi- and tridentate ʟ-Asn in Cu(ʟ-His)(ʟ-Asn) and Cu(ʟ-Asn)$_2$. Apart from that, they give new insights into the tridentate copper(II) binding in aqueous solution by detailing the exact structures, coordination modes and apically coordinated atoms.

Intramolecular hydrogen bonds. Yamauchi et al. stated an interesting hypothesis that the inter-ligand noncovalent inter-actions between the polar groups of ʟ-Thr, ʟ-Asn or ʟ-Gln with ʟ-His may be a factor governing the preferential formation of a ternary copper(II) complex in aqueous solutions.[32] They assumed that the interaction is formed between an apical O of ʟ-His in the H-mode and the amido or the hydroxyl group.

The previously reported analysis of the hydrogen bonds in the DFT/B3LYP gas-phase and aqueous conformers of Cu(ʟ-His)(ʟ-Thr) showed that, although a specific conformer suggested by Yamauchi et al. was among the lower-energy conformers, generally, the intermolecular interactions between the complex and water molecules did not promote the formation of inter-residual hydrogen bonding.[19] Instead, these interactions stabilized the conformers with intra-residual hydrogen bonds. To examine if the same conclusions are valid for the ʟ-Asn copper (II) complexes, the hydrogen bonds formed in Cu(ʟ-Asn)$_2$ and Cu(ʟ-His)(ʟ-Asn) in the gas phase and aqueous solution are analyzed (Tables S93–S95).

Like for Cu(ʟ-His)(ʟ-Thr),[19] the distribution of intramolecular hydrogen bonds presented in Tables S93 − S95 reveals a more pronounced abundance of intra- than inter-residual hydrogen bonds. The conformers with the inter-residual hydrogen bonds are rare; examples are tNONO1 (Figure 1) and cHNw1 (Figure 3). The Cu(ʟ-Asn)$_2$ conformers with inter-ligand bonding are not among the lower-energy ones, but cHNw1, that corresponds to the structure proposed by Yamauchi et al.,[32] is the only such Cu(ʟ-His)(ʟ-Asn) lower-energy conformer. The most common intra-ligand hydrogen bond is N$_{am}$–H···O$_{ad}$ in both environments (Tables S93–S95). Interestingly, this is the hydrogen bond of inter-residual type that occurs in the Asx turn in proteins.[68] However, in view of the larger number of aqueous than gas-phase conformers, another possible ʟ-Asn intra-residual hydrogen bond, N$_{ad}$–H···O$_c$, may be considered to be less frequent in aqueous solution than in the gas phase (Tables S93–S95). The intra-ligand hydrogen bonds were equally formed in the PCM structures of aqueous conformers without and with one and two explicit water molecules (Figure S8).

Although Cu(ʟ-His)(ʟ-Asn) has one more donor for hydrogen bonding than Cu(ʟ-His)(ʟ-Thr),[19] the difference between the numbers of hydrogen bonds realized in the gas phase and aqueous medium is less substantial for the former than for the latter ternary complex. Regarding the ʟ-His ligand, N$_{am}$–H···N$_{im}$ is the most often formed hydrogen bond in the glycinato-mode conformers (Table S95) of both ternary complexes. But, regarding the ʟ-Asn conformations, it seems that their stability in the title complexes is directed by forming N$_{am}$–H···O$_{ad}$ in the first place, and then by intermolecular interactions of –N$_{ad}$H$_2$ with water molecules. It appears that the conformational flexibility is

not so pronounced for the ʟ-His ternary complex with ʟ-Asn as for the complex with ʟ-Thr[19].

The supposition can be connected with the numbers of glycinato-mode conformers of the parent and ternary complexes. The gas-phase conformational analysis of Cu(ʟ-His)$_2$ resulted in 15 *trans* and 22 *cis* glycinato-mode conformers.[17] By comparing the numbers of glycinato-mode conformers of Cu(ʟ-Thr)$_2$[18] and Cu(ʟ-Asn)$_2$ in the gas phase, they are similar, 35 *trans* and 22 *cis* for the former, and 31 *trans* and 17 *cis* for the latter complex. In their ternary complexes with ʟ-His, the number of glycinato-mode conformers increased for both in the gas phase [50 *trans* and 52 *cis* for Cu(ʟ-His)(ʟ-Thr),[19] and 69 *trans* and 63 *cis* of Cu(ʟ-His)(ʟ-Asn)]. These results indicate the smaller steric hindrance in the ternary than in the parent binary complexes. Conversely to the gas phase, in aqueous solution, the total number of Cu(ʟ-His)(ʟ-Thr) conformers (158 *trans* and 153 *cis*)[19] is considerably larger than of the Cu(ʟ-His)(ʟ-Asn) ones (127 *trans* and 122 *cis*) as well as the number of conformers with $\Delta G_{water} \leq 10.0$ kJ mol^{-1} (80 vs. 57 for the ʟ-Thr[19] and ʟ-Asn ternary complexes, respectively). The larger number of PCM structures suggests that the ʟ-Thr side-chain hydroxyl group has a better adaptability than the ʟ-Asn amido group to the local aqueous surroundings.

2.4. The DFT/B3LYP Reproduction of the Experimental X-Ray Molecular Structures

In addition to the approach described above, the experimental X-ray crystal structures of Cu(ʟ-Asn)$_2$,[36] Cu(ʟ-His)(ʟ-Asn),[37] and [Cu(ʟ-His)(ʟ-Asn)(H$_2$O)·3H$_2$O][37] were used as the starting coordinates for geometry optimizations in the gas phase and in aqueous surroundings using PCM. The superposition of the resulting calculated and experimental structures is illustrated in Figures 8–10. The comparison between the gas-phase equilibrium geometries and the X-ray molecular structures could point to an impact of intermolecular interactions on the molecular geometry. Besides, the superposition of the PCM-estimated and crystalline geometries examines whether non-covalent interactions modeled by PCM can cause the same effect on the geometry changes as the crystal lattice does.

Cu(ʟ-Asn)$_2$. The coordination mode in the X-ray crystal structure is *trans*-NONO.[36] The compound has the side chains in an axial and an equatorial position with respect to the
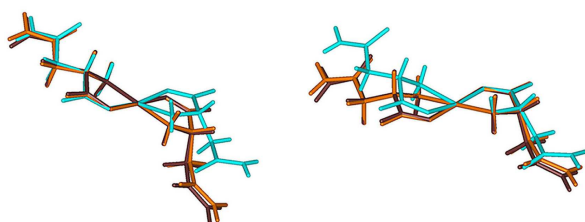
chelate rings, and N$_{am}$–C$^\alpha$–C$^\beta$–C$_{ad}$ ≈ −60°. In the crystal lattice, the copper(II) atom has two O$_{ad}$ atoms from adjacent complexes in the axial positions at 2.229(4) and 2.885(4) Å, and the pyramidal distortion of the coordination polyhedron.[36]
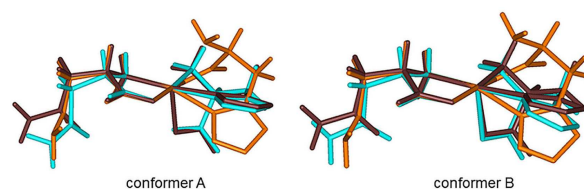
The superposition between the DFT equilibrium geometries and the experimental structure with respect to each of the chelate rings shows a good fit between the compared geometries (Figure 8). This indicates that the differences between the structures are mainly due to the copper(II) coordination polyhedron shape, which is much more distorted from planarity in the X-ray crystal structure than in the calculated ones. The result is in accord with previous comparisons between the crystalline and gas-phase geometries of Cu(aa)$_2$ that strain due to the crystal lattice effects can be alleviated by distortion of the copper(II) coordination geometry from planarity.[56] The crystalline conformation corresponds to the B3LYP axial-equatorial conformer named tNONO13 in the gas phase, and tNONOw8 in aqueous solution (Tables S2 and S39, respectively). The relative electronic energy of the conformer dropped from 25.3 kJ mol^{-1} in the gas phase to 6.1 kJ mol^{-1} in aqueous solution.

Cu(ʟ-His)(ʟ-Asn). In the anhydrous and aqua Cu(ʟ-His)(ʟ-Asn) crystals,[37] the coordination mode is *cis*-HN with an apically coordinated ʟ-His O atom.

The asymmetric unit of the X-ray crystal structure of anhydrous Cu(ʟ-His)(ʟ-Asn)[37] contains two conformers (named A and B) with the ʟ-Asn side chain in an equatorial position, but with the amido group differently oriented. Specifically, N$_{am}$–C$^\alpha$–C$^\beta$–C$_{ad}$ ≈ 60° in both structures, and C$^\alpha$–C$^\beta$–C$_{ad}$–O$_{ad}$ equals −20.4° and −52.9° in A and B, respectively.

B3LYP geometry optimizations for isolated molecules and by using PCM, started from structures A and B, resulted in the same corresponding minima (Figure 9). They are tIN1 (C$^\alpha$–C$^\beta$–C$_{ad}$–O$_{ad}$ = −76.1°; Figure S6) and cHNw2 (C$^\alpha$–C$^\beta$–C$_{ad}$–O$_{ad}$ = −27.1°, Figure S7). The PCM structure retains the crystalline *cis*-HN mode while the gas-phase one is different (tIN). cHNw2 belongs to the group of lower-energy PCM minima ($\Delta G_{water} = 3.1$ kJ mol^{-1}). Its geometry is between the A and B ones, i.e., it shows better agreement with the experimental ʟ-His ligand in B than A, while ʟ-Asn part is better matched with A than B (Figure 9).

The Cu(ʟ-His)(ʟ-Asn) geometry from the X-ray crystal structure of [Cu(ʟ-His)(ʟ-Asn)(H$_2$O)·3H$_2$O][37] has the ʟ-Asn side chain in an equatorial position (N$_{am}$–C$^\alpha$–C$^\beta$–C$_{ad}$ ≈ −60°, C$^\alpha$–C$^\beta$–C$_{ad}$–O$_{ad}$ = −17.6°). It was optimized with and without 4

Figure 8. Superposition of the Cu(ʟ-Asn)$_2$ structures with respect to each chelate ring. The experimental X-ray molecular structure[36] is denoted light blue, and the B3LYP estimated gas-phase and PCM aqueous equilibrium structures are orange and brown, respectively.

conformer A   conformer B

Figure 9. Superposition of the Cu(ʟ-His)(ʟ-Asn) structures for anhydrous conformers A and B from the X-ray crystal asymmetric unit.[37] The experimental molecular structures are marked light blue, while the B3LYP gas-phase and PCM aqueous structures are orange and brown, respectively.

H_2O (Figure 10). In the crystal structure,[37] the amido-group atoms form hydrogen bonds with surrounding water molecules, and an intermolecular N_{ad}—H···$O_{c,His}$ bond as well. During the [Cu(L-His)(L-Asn)(H_2O)·$3H_2O$] geometry optimization, the complex retained its initial *cis*-HN mode both in the gas phase and in aqueous environment. Without 4 H_2O, the gas-phase geometry optimization again yielded the coordination-mode change to *trans*-IN (tIN5, Figure S6, Table S78). By using PCM, the starting structure, either with or without 4 H_2O, converged to cHNw4 (C^α—C^β—C_{ad}—O_{ad} = 6.4°, Table S89), which fits well with the experimental crystalline structure (Figure 10). The deviation in the C^α—C^β—C_{ad}—O_{ad} angle may be attributed to the amido-group flexibility to accommodate the most efficient crystal packing. The cHNw4 conformer is the most stable one of the HN-mode conformers regarding the Gibbs free energy (Figure 3).

To sum up, all of the PCM structures obtained when starting from the crystal structures show quite good reproduction of the experimental crystalline molecular structures. This identification shows that the experimental structures are the conformers belonging to the groups of B3LYP-estimated lower-energy aqueous minima (tNONOw8 in Table 3; cHNw2 and cHNw4 in Table 4). This suggests that B3LYP and PCM can satisfactorily model the impact of noncovalent interaction on the geometry changes in the studied systems.

2.5. DFT/B3LYP Prediction of *g*-Factor and HFCC *A* Values

The DFT/B3LYP **g** tensor and HFCC **A** tensor were calculated for selected conformers of Cu(L-Asn)$_2$ and Cu(L-His)(L-Asn) with various combinations of the in-plane and apical donor atoms to examine their influence on the magnetic parameters. The calculated isotropic g_{iso} and the most variable g_z component of the **g** tensor, HFCC of the ^{63}Cu (A^{Cu}) and ^{14}N (A^N) centers were compared with their values obtained from the EPR spectra measured in aqueous solutions (Table 6).

Goodman et al. identified a mixture of *cis*- and *trans*-Cu(L-Asn)$_2$ with CuN_2O_2 equatorial coordination to simultaneously exist in aqueous solutions at room temperature by the EPR spectroscopy, and determined their A^{Cu}_{iso} and A^N_{iso} values (Table 6).[44,45] From the superhyperfine ^{14}N splitting in the EPR spectra, they determined two A^N_{iso} values for the two isomers, but their assignment to either *trans*- or *cis*-Cu(L-Asn)$_2$ was only tentative.[45] Our calculations for aqueous isomers of Cu(Gly)$_2$ (Table S96), and several conformers of Cu(L-Asn)$_2$ and Cu(L-His)(L-Asn) (Table 6) with the Cu^{II} coordination number (CN) 4, 5, or 6 suggest that the A^N_{iso} value is always larger for the *cis* than *trans* conformers with the same CN. This is in accord with the results reported by Pezzato et al. that the DFT/B3LYP calculated A^N_{iso} value is smaller for *trans*- than *cis*-Cu(Gly)$_2$·$2H_2O$ in implicitly modeled aqueous solution.[69]

The experimental g_{iso} values are underestimated for both Cu(L-Asn)$_2$ and Cu(L-His)(L-Asn), by 0.034 and 0.028 on average by our B3LYP calculations (Table 6), respectively. A similar underestimation of *g* values was also obtained for some other copper(II) complexes by Sciortino et al.[70]

In accord with the known fact that the presence of ligands in the axial positions causes an increase of g_z and a decrease of A_z,[70] our DFT/B3LYP results gave a ca. 40 MHz lower $|A^{Cu}_{iso}|$, a bit larger g_{iso} value, and slightly lower A^N_{iso} values for the conformers with intramolecular axial Cu-donor bond (CN = 5) than for the conformers with CN = 4, independently on the *cis*- or *trans*-configuration for all of the studied complexes (Tables 6 and S96).

To examine the influence of water molecules on the magnetic properties, the EPR parameters were also calculated for equilibrium structures of selected conformers with one and two explicit water molecules using PCM (Table 6). Although the conformer geometries without and with explicit water molecules differ owing to the hydrogen bonds with the explicit water molecules (Figure S8), their torsion angles are within the characteristic values for a specific conformer.

The apical coordination does not substantially influence the distribution of unpaired spin density since it resides in the metal atom and four in-plane ligand atoms (Figure S12). A water molecule in the apical position affects equally as an intramolecular apical donor atom the lowering of $|A^{Cu}_{iso}|$ (Tables 6 and S96). For the systems with two water molecules, the addition of the second H_2O to the calculations produced an extra lowering of $|A^{Cu}_{iso}|$ by ≈ 20 MHz, independently whether this H_2O was in the apical position or in the second Cu^{II} coordination sphere (Table 6). Nevertheless, an exceptional case is the tGNw3_b·$2H_2O$ equilibrium structure (Figure 11). For that system, with an H_2O in the apical position, and a second H_2O forming two hydrogen bonds in the equatorial plane, $|A^{Cu}_{iso}|$ is lowered by 35 MHz relatively to the systems with one explicit H_2O (Figure 11).

Generally, the structures obtained in implicitly modeled aqueous solution represent an average of all possible geometries that a specific conformer can attain under the influence of noncovalent interactions with surrounding water molecules. Adding explicit water molecules in the PCM calculations gave insight into how changes in a local aqueous environment could affect the changes in the conformer geometry. Generally, the Cu^{II} coordination geometry in the examined conformers is more distorted from planarity when explicit water molecules are considered. In the tGNw3 systems (Figure 11), O—Cu—O' is 178.9° in tGNw3, 174.1° in tGNw2_a1, 178.9° in tGNw2_a2, and 161.7° in tGNw3_b. To separate the effect of an apical H_2O coordination from that of a distorted geometry, the *g* and *A* values were calculated for the conformers from the equilibrium
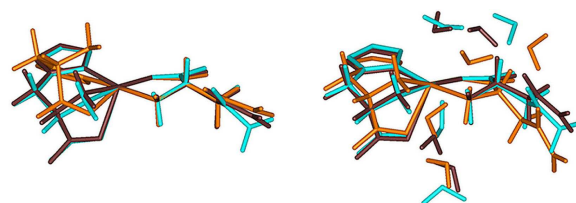
Figure 10. Superposition of the Cu(L-His)(L-Asn) (left) and [Cu(L-His)(L-Asn)(H_2O)·$3H_2O$] structures (right). The experimental X-ray molecular structure[37] is light blue, and the B3LYP gas-phase and PCM aqueous ones are orange and brown, respectively.

Table 6. DFT/B3LYP magnetic parameters, g_{iso}, g_z, and HFCC A_{iso} (MHz), A_x (MHz), A_y (MHz), A_z (MHz) of the ^{63}Cu and coordinating ^{14}N centers calculated in implicitly modeled aqueous solution for denoted conformers of Cu(L-Asn)$_2$ with CuN$_2$O$_2$ equatorial coordination, and Cu(L-His)(L-Asn) without and with up to two explicit water molecules.[a]

Structure	g_{iso}	g_{zz}	A^{Cu}_{iso}	A^{Cu}_x	A^{Cu}_y	A^{Cu}_z	A^N_{iso}	apical donor atom(s)
Cu(L-Asn)$_2$[b]								
tNONOw1	2.078	2.148	−242.2	−42.4	−59.3	−624.9	29.9 (N$_{am}$), 30.1 (N$_{am}'$)	-
tNONOw1_a1·H$_2$O	2.089	2.165	−203.1	−1.8	−11.1	−596.3	28.7 (N$_{am}$), 29.7 (N$_{am}'$)	O$_{water}$
tNONOw1_a2·H$_2$O	2.088	2.164	−201.9	−2.2	−8.6	−595.1	28.6 (N$_{am}$), 29.6 (N$_{am}'$)	O$_{water}$
tNONOw1_b·2H$_2$O	2.096	2.176	−180.7	20.3	21.0	−583.4	28.5 (N$_{am}$), 27.7 (N$_{am}'$)	2 O$_{water}$
tNONOw1_b	2.081	2.154	−236.4	−39.8	−55.7	−613.7	29.2 (N$_{am}$), 28.8 (N$_{am}'$)	-
tNONOw2	2.090	2.166	−198.1	6.1	−8.9	−591.5	28.2 (N$_{am}$), 29.6 (N$_{am}'$)	O$_{ad}$
tNONOw2_a·H$_2$O	2.090	2.167	−183.6	−8.8	33.5	−575.5	27.3 (N$_{am}$), 28.9 (N$_{am}'$)	O$_{ad}$
tNONOw2_a	2.090	2.167	−191.6	−12.4	21.0	−583.4	27.4 (N$_{am}$), 28.9 (N$_{am}'$)	O$_{ad}$
tNONOw6	2.090	2.166	−199.2	5.4	−10.5	−592.5	28.6 (N$_{am}$), 29.8 (N$_{am}'$)	O$_{ad}$
tNONOw10	2.078	2.148	−243.1	−42.8	−60.6	−626.0	30.7 (N$_{am}$), 30.7 (N$_{am}'$)	-
cNONOw1	2.091	2.168	−205.1	−7.2	−10.5	−597.6	31.8 (N$_{am}$), 32.3 (N$_{am}'$)	O$_{ad}$
cNONOw2	2.078	2.149	−245.2	−54.5	−54.9	−626.3	33.7 (N$_{am}$), 33.7 (N$_{am}'$)	-
cNONOw2_a·H$_2$O	2.089	2.166	−203.6	−1.4	−13.1	−596.2	32.2 (N$_{am}$), 32.2 (N$_{am}'$)	O$_{water}$
cNONOw2_b·2H$_2$O	2.096	2.176	−185.0	13.8	17.5	−586.3	31.1 (N$_{am}$), 31.0 (N$_{am}'$)	2 O$_{water}$
cNONOw2_b	2.082	2.155	−240.7	−52.1	−52.8	−617.2	32.4 (N$_{am}$), 32.7 (N$_{am}'$)	-
cNONOw6	2.078	2.149	−245.2	−54.3	−55.1	−626.2	33.8 (N$_{am}$), 34.1 (N$_{am}'$)	-
tNONOw43	2.082	2.155	−230.8	−30.6	−44.5	−617.5	29.4 (N$_{am}$), 30.7 (N$_{am}'$)	N$_{ad}$
tNONow1	2.098	2.179	−97.3	15.8	171.3	−480.5	27.0 (N$_{am}$), 26.8 (N$_{am}'$)	O
tNONow2	2.099	2.180	−98.8	10.5	176.7	−481.7	27.2 (N$_{am}$), 27.2 (N$_{am}'$)	O
tNONow3	2.108	2.193	−68.5	41.8	211.9	−459.3	26.4 (N$_{am}$), 26.7 (N$_{am}'$)	O; O$_{ad}$
cNONow1	2.100	2.179	−96.2	−8.5	185.6	−465.8	28.5 (N$_{am}$), 36.0 (N$_{am}'$)	O
Cu(L-His)(L-Asn)[c]								
tGNw1	2.095	2.175	−172.5	9.7	39.3	−566.7	28.0 (N$_{am}$), 29.1 (N$_{am}'$)	N$_{im}$
tGNw1_a·H$_2$O	2.097	2.177	−155.4	9.6	70.4	−546.3	27.7 (N$_{am}$), 28.4 (N$_{am}'$)	N$_{im}$
tGNw1_a	2.097	2.177	−159.8	9.1	62.5	−551.0	27.8 (N$_{am}$), 28.6 (N$_{am}'$)	N$_{im}$
tGNw3	2.075	2.144	−249.7	−47.8	−75.8	−625.6	32.2 (N$_{am}$), 31.6 (N$_{am}'$)	-
tGNw3_a1·H$_2$O	2.089	2.165	−202.1	−2.1	−8.2	−595.9	29.1 (N$_{am}$), 29.1 (N$_{am}'$)	O$_{water}$
tGNw3_a2·H$_2$O	2.088	2.164	−201.9	−1.5	−9.3	−594.8	28.4 (N$_{am}$), 28.4 (N$_{am}'$)	O$_{water}$
tGNw3_b·2H$_2$O	2.093	2.170	−167.1	−9.5	67.3	−559.1	28.2 (N$_{am}$), 28.3 (N$_{am}'$)	O$_{water}$
tGNw3_b	2.083	2.157	−219.7	−24.2	−40.8	−594.2	28.5 (N$_{am}$), 27.2 (N$_{am}'$)	-
cGNw3	2.097	2.177	−178.5	4.8	30.8	−571.0	31.7 (N$_{am}$), 32.2 (N$_{am}'$)	N$_{im}$
cGNw5	2.091	2.168	−205.6	−7.3	−11.5	−598.1	31.9 (N$_{am}$), 32.0 (N$_{am}'$)	O$_{ad}$
cHNw1	2.091	2.167	−187.5	−18.2	37.6	−582.0	30.2 (N$_{am}$), 39.8 (N$_{im}$), 33.3 (N$_{am}'$)	O$_{His}$

Table 6. continued

Structure	g_{iso}	g_{zz}	A^{Cu}_{iso}	A^{Cu}_x	A^{Cu}_y	A^{Cu}_z	A^N_{iso}	apical donor atom(s)
cHNw4	2.091	2.166	−185.8	10.4	14.3	−582.1	32.6 (N_{am}), 38.1 (N_{im}), 33.6 (N_{am}')	O_{His}
cHNw4_a·H_2O	2.097	2.175	−170.2	23.7	39.9	−574.3	31.4 (N_{am}), 37.0 (N_{im}), 32.8 (N_{am}')	O_{His}; O_{water}
cHNw4_a	2.089	2.165	−199.4	1.4	−8.8	−590.7	32.6 (N_{am}), 38.0 (N_{im}), 33.6 (N_{am}')	O_{His}
tHNw1	2.092	2.168	−166.5	−12.4	71.9	−559.1	31.3 (N_{am}), 37.4 (N_{im}), 30.3 (N_{am}')	O_{His}
tINw1	2.100	2.184	−163.0	11.8	52.5	−553.2	33.7 (N_{im}), 31.7 (N_{am}')	$N_{am,His}$
cINw1	2.101	2.186	−164.7	18.1	41.3	−553.6	36.7 (N_{im}), 33.3 (N_{am}')	$N_{am,His}$

[a] The conformers in the equilibrium structures with one or two explicit water molecules have letter "a" (one H_2O) or "b" (two H_2O) in the name (Figure S8). Their magnetic parameters were obtained by the single point calculations on these equilibrium structures as well as on the _a and _b conformers taken from the equilibrium structures without accounting the explicit water molecule(s). [b] Experimental g-factor and HFCC A values from the EPR spectra measured at pH $\approx$ 7 at (i) room temperature in aqueous solution:[45] $|A^{Cu}_{iso}| = 199$ MHz and $A^N_{iso} = 28.3$ MHz for one isomer, and $|A^{Cu}_{iso}| = 165$ MHz and $A^N_{iso} = 25.5$ MHz for other isomer (assigned tentatively to trans and cis, respectively) and (ii) at 77 K in frozen solution:[47] $g_\perp = 2.055$, $g_{||} = 2.258$, $A^{Cu}_\perp = −70.1$ MHz, $A_{||} = −510.7$ MHz, $A^N_\perp = 29.4$ MHz, $A^N_{||} = 25.2$ MHz; the isotropic $g_{iso} = 2.123$, and $A^{Cu}_{iso} = −216.8$ MHz, $A^N_{iso} = 27.8$ MHz were calculated by means of experimental $g_\perp$, $g_{||}$, $A_\perp$, and $A_{||}$ using the equations given elsewhere.[47] [c] Experimental g-factor and HFCC A values (given as absolute values) from the EPR spectrum measured at 133 K in frozen solution:[46] $g_\perp = 2.060$, $g_{||} = 2.238$, $g_{iso} = 2.120$, $|A^{Cu}_{iso}| = 218.8$ MHz, $|A_{||}| = 590.6$ MHz.

systems with explicit water molecules, but without accounting the explicit H_2O. The resulting values (Table 6) show that indeed
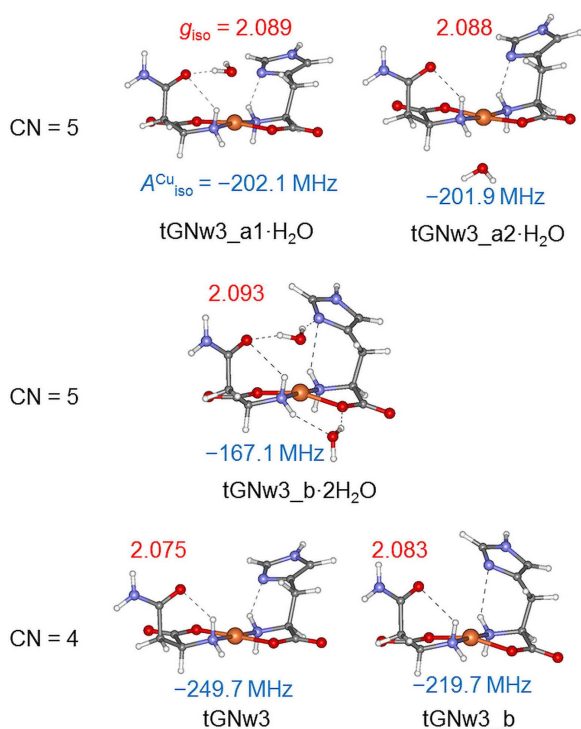
Figure 11. The predicted g_{iso} (red) and A^{Cu}_{iso} (blue) values for the aqueous tGNw3 systems without and with explicit water molecules. CN stands for the copper(II) coordination number. tGNw3_b (CN = 4) is the conformer taken from the tGNw3_b·$2H_2O$ equilibrium structure; its magnetic parameters were calculated by means of the single point calculation without two explicit water molecules.

A^{Cu}_{iso} is very much sensitive to the changes in the Cu^{II} coordination geometry. The changes are more pronounced for Cu(L-His)(L-Asn) than Cu(L-Asn)$_2$ (Table 6). Slightly different geometries of the same conformer produce more or less different A^{Cu}_{iso} values, dependently on the extent of the Cu^{II} coordination geometry distortion from planarity. For instance, the experimental $|A^{Cu}_{iso}|$ value (218.8 MHz)[46] is closer to the predicted value of more distorted tGNw3_b than less distorted tGNw3 (Figure 11, Table 6).

For Cu(L-His)(L-Asn), the HFCC anisotropic and isotropic components were determined for ^{63}Cu from the EPR spectrum measured in a water-glycerol solution at pH 7.5 − 8.0 and 133 K (Table 6).[46] Cocetta et al. assumed it likely that L-His adopted the H-mode with the CuN$_3$O chromophore in the ternary complex.[46] Nevertheless, the experimental HFCC values show the best fit with the calculated A^{Cu}_z and A^{Cu}_{iso} of the cHNw4, tGNw3, and cGNw5 conformers with apically positioned oxygen atom(s) (Table 6). This additionally proves that trans- and cis-Cu (L-His)(L-Asn) with both amino acids in the glycinato mode are present in aqueous solution at physiological pH.

For Cu(L-Asn)$_2$, the A^{Cu} values of the NONO conformers are quite similar, while those of the NONo conformers are different from the experimental values (Table 6). This furthermore verifies that only NONO conformers dominate in aqueous solution at physiological pH. A smaller A^N_{iso} is calculated for the trans than cis NONO conformers (Table 6), while the B3LYP A^{Cu}_{iso} values are very similar for the trans and cis conformers with the same CN. Our EPR interpretation points to the conclusion that in aqueous solution, a water molecule can place itself at the apical Cu^{II} position if it is free. Since Goodman et al. adjoined a smaller A^{Cu}_{iso} with a smaller A^N_{iso} constant for either trans- or cis-isomer of Cu(L-Asn)$_2$,[45] it may be that tNONO and cNONO conformers

have more often a CN equal to 6 and 5, respectively, in aqueous solution at room temperature.

3. Conclusions

Comparisons between the experimental X-ray molecular structures of Cu(L-Asn)$_2$ and Cu(L-His)(L-Asn) with their corresponding DFT-calculated gas-phase and aqueous equilibrium structures show that B3LYP using PCM can simulate the noncovalent interactions in the studied complexes well.

The DFT exact structures, coordination modes, bi- or tridentate binding, and magnetic parameters determined for the title complexes in aqueous solution enabled the confirmation and, for apical bonding, also the refinement of structural predictions from literature.

For both Cu(L-Asn)$_2$ and Cu(L-His)(L-Asn), the *trans* glycinato-mode conformers are the most stable ones in the gas phase. The conformational analysis of Cu(L-Asn)$_2$ in aqueous solution confirmed the glycine-like mode to be prevailing, both in the *trans* and *cis* configuration, in accord with the interpretations of experimental results (detailed in the Introduction). In aqueous solution, the ternary Cu(L-His)(L-Asn) complex has many lower-energy conformers in different coordination modes with $\Delta G_{water} \leq 10.0 \ kJ\,mol^{-1}$, but the *trans* and *cis* GN and HN are the prevailing ones.

The analysis of the apical copper-donor distances in the title complexes showed that the tridentate–bidentate amino-acid binding dominates in the lower-energy aqueous conformers. L-His is more often found than L-Asn tridentate in such Cu(L-His)(L-Asn) geometries, which is in accordance with the experimental studies[40,41] that suggested L-His to be tridentate, and L-Asn to have a transient tridentate binding. However, compared to the structural proposals in literature, which predicted L-His to be only in the H mode with the O atom apically positioned, the DFT/B3LYP prediction is that the lower-energy conformers with L-His in the G and I modes with apical N_{im} and N_{am}, respectively, are also possible in aqueous solution. This does not contradict the tridentate L-His experimental finding. The match between the experimental[46] and DFT predicted A^{Cu}_z and A^{Cu}_{iso} reveals that the tGN, cGN, and cHN conformers with an apical oxygen atom (either intramolecular or from a water molecule) could be in a frozen aqueous solution during the EPR measurement.

The analysis of the hydrogen bonds formed in the title complexes revealed a high tendency for forming an intra-residual N_{am}—H···O_{ad} in the L-Asn ligand. This tendency stereochemically restricts the $—N_{ad}H_2$ group in the hydrogen bond formation.

Compared to Cu(L-His)(L-Thr),[19] the intermolecular interactions between Cu(L-His)(L-Asn) and aqueous environment do not have a pronounced effect on forming the intra-residual hydrogen bonds like they had in the former complex. It seems that in the Cu^{II} ternary complex with L-His, the L-Thr hydroxyl group is superior to the L-Asn amido group to adapt to changes in local aqueous surroundings. Although both ternary complexes have a similar number of gas-phase conformers, a smaller number of aqueous conformers of Cu(L-His)(L-Asn) than

Cu(L-His)(L-Thr) supports the supposition. Since the simulation of the Cu^{II} distribution in the ultrafiltrable fraction of normal blood plasma yielded a much larger percentage of ultrafiltrable Cu^{II} in Cu(L-His)(L-Thr) than in Cu(L-His)(L-Asn),[51] it may be that there is a connection between the conformational flexibility and adaptability to the local surroundings and the abundance of the copper(II)-L-His ternary complexes in physiological conditions.

Computational Methods

Constructing Initial Structures for Geometry Optimization

Cu(L-Asn)$_2$. After defining 15 *trans* and 15 *cis* in-plane coordination modes (see 2.1), the initial structures for each of them were generated as follows:

NO mode. L-Asn bound to the copper(II) forms a five-member ring with C^α slightly above or below the plane of the other four atoms; as a result, C^β is either in an axial or an equatorial position to the ring. Three orientations per full rotation of the bond $C^\alpha—C^\beta$ were assumed with $C_{ad}—C^\beta—C^\alpha—N_{am}$ torsion values of 60°, −60° and 180°. For the amide group, seven orientations were used to construct initial geometries, with $O_{ad}=C_{ad}—C^\beta—C^\alpha$ torsions of −120°, −75°, −30°, 15°, 60°, 105° and 150° (these values were determined in a preliminary series of geometry optimizations). In the NONO mode of Cu(L-Asn)$_2$, combining 21 axial and 21 equatorial conformations of L-Asn in the complex leads to 903 *trans* and 903 *cis* unique initial structures.

Oo mode. By binding L-Asn to the copper(II) via O and O_{ad}, a seven-member ring is formed. A preliminary series of calculations indicated twelve combinations of torsion angles quadruplets of Cu—O—C_c—C^α, O—C_c—C^α—C^β, C_c—C^α—C^β—C_{ad}, and C^α—C^β—C_{ad}—O_{ad}, which were used to generate initial structures: {100°, −60°, 0°, 60°}, {10°, −60°, 0°, 60°}, {60°, −60°, −20°, 80°}, {0°, −60°, 120°, −60°}, {0°, −90°, 90°, 0°}, {90°, −90°, 0°, 60°}, {−100°, 60°, 0°, −60°}, {−10°, 60°, 0°, −60°}, {−60°, 60°, 20°, −80°}, {0°, 60°, −120°, 60°}, {0°, 90°, −90°, 0°}, and {−90°, 90°, 0°, −60°}. For OoOo, this resulted in a total of 78 unique *cis* and 78 unique *trans* combinations.

On mode. This mode construction was identical to the Oo mode, except that the last torsion angle is C^α—C^β—C_{ad}—N_{ad} instead of C^α—C^β—C_{ad}—O_{ad}.

Nn mode. The binding of L-Asn to the copper(II) forms a six-member ring. A preliminary series of calculations indicated eight combinations of the Cu—N_{am}—C^α—C^β, N_{am}—C^α—C^β—C_{ad} and C^α—C^β—C_{ad}—N_{ad} angles that were used to generate initial structures: {60°, −60°, 60°}, {−60°, 60°, −60°}, {0°, −60°, 0°}, {0°, 60°, 0°}, {30°, −70°, 10°}, {−30°, 70°, −10°}, {60°, −60°, 10°}, and {−60°, 60°, −10°}. For the NnNn coordination mode, this resulted in a total of 36 unique *cis* and 36 unique *trans* combinations.

No mode. As above, this mode construction is identical to the Nn one except that the last torsion is C^α—C^β—C_{ad}—O_{ad} instead of C^α—C^β—C_{ad}—N_{ad}.

Mixed binding modes. We applied the structural principles outlined above for each mode, with *cis* and *trans* connectivity. By doing so, we created the initial structures in the mixed coordination modes, as follows: 432 NOOo, 288 NONo, 44 NONn, 432 NOOn, 192 NnOn, 192 NnOo, 156 OnOo, 144 NnNo, 192 NoOo, and 192 NoOn.

Initial structures of Cu(L-His)(L-Asn). To construct the initial structures of Cu(L-His)(L-Asn), the L-His initial conformations were

combined with the ʟ-Asn NO-mode initial structures. The construction of ʟ-His conformations in the five-member G and Gp, six-member H, and seven-member I chelate-ring geometries was based on the conformational analyses of Cu(ʟ-His)$_2$ and Cu(ʟ-His)(ʟ-Thr) described elsewhere.[17,19]

DFT Calculations

Conformational analyses. Both Cu(ʟ-Asn)$_2$ and Cu(ʟ-His)(ʟ-Asn) are electrically neutral molecules with a spin multiplicity of 2. The equilibrium structures of Cu(ʟ-Asn)$_2$ and Cu(ʟ-His)(ʟ-Asn) were optimized using the unrestricted DFT method with the B3LYP hybrid density functional[20–23] using the LanL2DZ double-ζ basis set,[71] which was additionally augmented by a set of polarization[72] and diffuse functions[73] on N, O, and C atoms. The nonrelativistic effective-core potentials of Hay and Wadt[74–76] were used to describe the shielding effects of electrons in the copper inner shells. The suitability of the method/basis set for the conformational analyses of Cu(aa)$_2$ complexes was extensively evaluated elsewhere.[17–19,54] Besides, the application of this combination of functional and basis set, which was previously applied for the conformational analyses of physiological Cu(ʟ-His)$_2$,[17] Cu(ʟ-Thr)$_2$,[18] and Cu(ʟ-His)(ʟ-Thr),[19] allows a comparison of the new results estimated for the title complexes with the previously studied systems at a consistent level.

The equilibrium geometries were computed for the conformers of Cu(ʟ-Asn)$_2$ and Cu(ʟ-His)(ʟ-Asn) both in the gas phase and in a simulated aqueous environment. Additionally, several conformers of Cu(ʟ-Asn)$_2$ and Cu(ʟ-His)(ʟ-Asn), and cis- and trans-Cu(Gly)$_2$, were geometry optimized with one and two explicit water molecules initially placed at the apical position(s) to the copper(II), together with implicitly modeled aqueous solution using PCM. All conformers were verified by frequency calculations to have no imaginary frequencies. Implicit solvent effects (the dielectric constant for water $\varepsilon = 78.39$) were modeled with the integral equation formalism of polarizable continuum model (PCM)[52,53,77] as it is implemented in Gaussian 09 suite of programs[78] (SCRF=PCM) and detailed elsewhere.[77] The solute cavity was created via a set of overlapping spheres using the UFF atomic radii,[79] scaled by a factor of 1.1, and the density of surface elements was set to 5/Å^2. The correctness of applying PCM for conformational analysis in aqueous solution was confirmed by comparing the results acquired by the PCM calculations of sole Cu(ʟ-His)(ʟ-Thr) and for a few Cu(ʟ-His)(ʟ-Thr) conformers surrounded by 20 explicit water molecules.[19] The thermal correction to the Gibbs free energy was calculated at a temperature of 298.15 K in the standard way. All calculations were carried out with the Gaussian 09 suite of programs.[78]

Magnetic parameters for EPR spectra. The **g** tensor and **A** tensor for selected conformers of Cu(ʟ-Asn)$_2$ and Cu(ʟ-His)(ʟ-Asn) without and with one or two explicit water molecules were calculated with the program ORCA[80,81] using B3LYP, a Wachters' basis set (62111111/3311111/3111) for Cu,[82] and the 6–311+G(d,p) basis set for the other atoms (H, C, N, O). This functional/basis set combination accurately predicted the ^{13}C and ^{1}H Fermi contact shifts for solid-state Cu(aa)$_2$ complexes.[61] The conductor-like polarizable continuum model (CPCM) was applied to account for solvent effects in aqueous solution. For the **g** tensor, the origin was set to the copper atom. The **A** tensor was obtained as a sum of three contributions as follows: the isotropic Fermi contact, the anisotropic dipolar and the spin-orbit coupling terms. The isotropic A_{iso} and g_{iso} values were calculated as an average of the anisotropic components A_x, A_y, A_z and g_x, g_y, g_z, respectively.

As a benchmark, we tested the [Cu(H$_2$O)$_6$]$^{2+}$ and trans- and cis-Cu(Gly)$_2$ systems, and compared their magnetic properties (g_{iso}, and HFCC of copper and nitrogen, A^{Cu}_{iso} and A^N_{iso}, respectively) with available experimental data. The [Cu(H$_2$O)$_6$]$^{2+}$ structure was taken without further optimization from the literature.[83] Since B3LYP and PBE0[84,85] were reported to give good magnetic properties for several copper(II) complexes with the lowest mean absolute percent deviation of less than 3.5% for g_z (PBE0), and 9.5% for A_z (B3LYP),[70] we tested these two DFT functionals with different basis sets for copper [including def2-TZVP, Wachters' basis for Cu with and without f-functions, and Pople's 6-311G(d,p) basis set]. For the [Cu(H$_2$O)$_6$]$^{2+}$ complex, PBE0 performed better, but for Cu(Gly)$_2$, the B3LYP functional with the Wachters' Cu basis set showed better agreement with experimental EPR parameters.[47,69,86] Therefore, in this study, the method combination B3LYP/Wachters(Cu)/6-311+G (d,p)(C,N,O)/6-31G(d)(H) was chosen to calculate the magnetic parameters and evaluate the structure-magnetic property relation of the title Cu(aa)$_2$ complexes.

Calculating Statistical Weight of a Conformer and Weighted Average of ΔG_{water}

The statistical weight of the jth conformer, w_j, is given as a weighted average from the Boltzmann distribution of all conformers as follows:

$$\Delta G_{water,j} = G_{water,j} - G_{water,min}$$

$$w_j = \exp(-\Delta G_{water,j}/RT)/\sum_i \exp(-\Delta G_{water,i}/RT]) \qquad (1)$$

where $G_{water,j}$ is the Gibbs free energy of the jth conformer in aqueous solution, $G_{water,min}$ is the lowest Gibbs free energy, R is the gas constant, T is a temperature (298.15 K), and the summation i goes over the conformers found in aqueous solution.

The weighted average of the relative Gibbs free energy in aqueous solution, $<\Delta G_{water}>$, is calculated from the Boltzmann distribution of accounted conformers:

$$< \Delta G_{water} > = \sum_i \Delta G_{water,i} \exp(-\Delta G_{water,i}/RT)/$$
$$\sum_i \exp(\Delta G_{water,i}/RT) \qquad (2)$$

Conflict of Interest

The authors declare no conflict of interest.

[1] M. C. Linder, *Biochemistry of copper; Series: Biochemistry of the Elements, Vol. 10*, Springer Science + Business Media: New York, **1991**.

[2] R. A. Festa, D. J. Thiele, *Curr. Biol.* **2011**, *21*, R877–R883.

[3] H. Kodama, C. Fujisawa, *Metallomics* **2009**, *1*, 42–52.

[4] F. Tisato, C. Marzano, M. Porchia, M. Pellei, C. Santini, *Med. Res. Rev.* **2010**, *30*, 708–749.

[5] M. C. Linder, *Metallomics*, **2016**, *8*, 887–905.

[6] P. Z. Neumann, A. Sass-Kortsak, *J. Clin. Invest.* **1967**, *46*, 646–658.

[7] B. Sarkar, T. P. Kruck, *Biochem. Cell Biol.* **1967**, *45*, 2046–2049.

[8] P. Deschamps, P. P. Kulkarni, M. Gautam-Basak, B. Sarkar, *Coord. Chem. Rev.* **2005**, *249*, 895–909.

[9] B. Sarkar, *Chem. Rev.* **1999**, *99*, 2535–2544.

[10] A. Garnica, W. Y. Chan, O. Rennert, *J. Pediatr.* **1994**, *125*, 336–338.

[11] H. Kodama, Y. Murata, M. Kobayashi, *Pediatr. Int.* **1999**, *41*, 423–429.

[12] C. Santini, M. Pellei, V. Gandin, M. Porchia, F. Tisato, C. Marzano, *Chem. Rev.* **2014**, *114*, 815–862.

[13] R. Tabti, N. Tounsi, C. Gaiddon, E. Bentouhami, L. Désaubry, *Med. Chem.* **2017**, *7*, 875–879.

[14] J. Gažo, I. B. Bersuker, J. Garaj, M. Kabešová, J. Kohout, H. Langfelderová, M. Melník, M. Serátor, F. Valach, *Coord. Chem. Rev.* **1976**, *19*, 253–297.

[15] B. Murphy, B. Hathaway, *Coord. Chem. Rev.* **2003**, *243*, 237–262.

[16] M. A. Halcrow , *Chem. Soc. Rev.* **2013**, *42*, 1784–1795.

[17] M. Marković, M. Ramek, J. Sabolović, *Eur. J. Inorg. Chem.* **2014**, 198–212.

[18] M. Marković, M. Ramek, C. Loher, J. Sabolović, *Inorg. Chem.* **2016**, *55*, 7694–7708.

[19] M. Ramek, M. Marković, C. Loher, J. Sabolović, *Polyhedron* **2017**, *135*, 121–133.

[20] A. D. Becke, *J. Chem. Phys.* **1993**, *98*, 5648–5652.

[21] C. Lee, W. Yang, R. G. Parr, *Phys. Rev. B* **1988**, *37*, 785–789.

[22] S. H. Vosko, L. Wilk, M. Nusair, *Can. J. Phys.* **1980**, *58*, 1200–1211.

[23] P. J. Stephens, F. J. Devlin, C. F. Chabalowski, M. J. Frisch, *J. Phys. Chem.* **1994**, *98*, 11623–11627.

[24] S. Dong, J. A. Ybe, M. H. Hecht, T. G. Spiro , *Biochemistry* **1999**, *38*, 3379–3385.

[25] F. Musiani, P. Carloni, S. Ciurli, *J. Phys. Chem. B* **2004**, *108*, 7495–7499.

[26] S. Sinnecker, F. Neese, *J. Comput. Chem.* **2006**, *27*, 1463–1475.

[27] M. C. White, F. D. Baker, R. L. Chaney, A. M. Decker, *Plant Physiol.* **1981**, *67*, 301–310.

[28] A. S. Krall, S. Xu, T. G. Graeber, D. Braas, H. R. Christofk, *Nat. Commun.* **2016**, *7*, 11457.

[29] S. R. V. Knott, E. Wagenblast, S. Khan, S. Y. Kim, M. Soto, M. Wagner, M.-O. Turgeon, L. Fish, N. Erard, A. L. Gable, A. R. Maceli, S. Dickopf, E. K. Papachristou, C. S. D'Santos, L. A. Carey, J. E. Wilkinson, J. C. Harrell, C. M. Perou, H. Goodarzi, G. Poulogiannis, G. J. Hannon, *Nature*, **2018**, *554*, 378–381.

[30] E. J. Baran, I. Viera, M. H. Torre, *Spectrochim. Acta* **2007**, *66A*, 114–117.

[31] Y. Saito, J. Odo, Y. Tanaka, *Chem. Pharm. Bull.* **1981**, *29*, 907–912.

[32] O. Yamauchi, T. Sakurai, A. Nakahara, *J. Am. Chem. Soc.* **1979**, *101*, 4164–4172.

[33] S. Misumi, I. Toshiyuki, S. Kimoto, *Bull. Chem. Soc. Jpn.* **1972**, *45*, 2695–2697.

[34] H. W. Richardson, J. R. Wasson, W. E. Estes, W. E. Hatfield, *Inorg. Chim. Acta* **1977**, *23*, 205–209.

[35] M. Fujimoto, *Bioinorg. Chem.* **1974**, *3*, 295–304.

[36] I. Vencato, C. Lariucci, K. D. Ferreira, R. C. Santana, J. F. Carvalho, *Acta Crystallogr. Sect. E* **2004**, *E60*, m1428–m1430

[37] T. Ono, H. Shimanouchi, Y. Sasada, T. Sakurai, O. Yamauchi, A. Nakahara, *Bull. Chem. Soc. Jpn.* **1979**, *52*, 2229–2234.

[38] J. H. Ritsma, G. A. Wiegers, F. Jellinek, *Recl. Trav. Chim. Pays-Bas* **1965**, *84*, 1577–1584.

[39] A. C. Baxter, D. R. Williams, *J. Chem. Soc. Dalton Trans.* **1974**, 1117–1120.

[40] A. Baxter, D. R. Williams, *J. Chem. Soc. Dalton Trans.* **1975**, 1757–1761.

[41] A. Gergely, I. Nagypál, E. Farkas, *J. Inorg. Nucl. Chem.* **1975**, *37*, 551–555.

[42] D. S. Barnes, L. D. Pettit, *J. Inorg. Nucl. Chem.* **1971**, *33*, 2177–2184.

[43] N. C. Li, E. Doody, J. M. White, *J. Am. Chem. Soc.* **1958**, *80*, 5901–5903.

[44] B. A. Goodman, D. B. McPhail, H. K. J. Powell, *J. Chem. Soc. Dalton Trans.* **1981**, 822–827.

[45] B. A. Goodman, D. B. McPhail, *J. Chem. Soc. Dalton Trans.* **1985**, 1717–1718.

[46] P. Cocetta, S. Deiana, L. Erre, C. Micerat, P. Piu, *J. Coord. Chem.* **1983**, 12, 213–218.

[47] T. Szabó-Plánka, A. Rockenbauer, M. Györ, F. Gaizer, *J. Coord. Chem.* **1988**, *17*, 69–83.

[48] K. M. Wellman, T. G. Mecca, W. Mungall, C. R. Hare, *J. Am. Chem. Soc.* **1968**, *31*, 805–807.

[49] F. Jursík, B. Hajék, *Collect. Czech. Chem. Commun.* **1973**, *38*, 2739–2746.

[50] I. Nagypál, E. Farkas, A. Gergely, *J. Inorg. Nucl. Chem.* **1975**, *37*, 2145–2149.

[51] V. Brumas, N. Alliey, G. Berthon, *J. Inorg. Biochem.* **1993**, *52*, 287–296.

[52] J. Tomasi, B. Mennucci, R. Cammi, *Chem. Rev.* **2005**, *105*, 2999–3094.

[53] B. Mennucci, *WIREs Comput. Mol. Sci.* **2012**, *2*, 386–404.

[54] J. Sabolović, M. Ramek, M. Marković, *J. Mol. Model.* **2017**, *23*, 290.

[55] D. R. Williams, *J. Chem. Soc. Dalton Trans.* **1972**, 790–797.

[56] J. Sabolović, K. R. Liedl, *Inorg. Chem.* **1999**, *38*, 2764–2774.

[57] O. M. D. Lutz, C. B. Messner, T. S. Hofer, M. Glätzle, C. W. Huck, G. K. Bonn, B. M. Rode, *J. Phys. Chem. Lett.* **2013**, *4*, 1502–1506.

[58] J. Sabolović, V. Gomzi, *J. Chem. Theory Comput.* **2009**, *5*, 1940–1954.

[59] M. Marković, N. Judaš, J. Sabolović, *Inorg. Chem.* **2011**, *50*, 3632–3644.

[60] M. Marković, D. Milić, J. Sabolović, *Cryst. Growth Des.* **2012**, *12*, 4116–4129.

[61] J. Pejić, D. Vušak, G. Szalontai, B. Prugovečki, D. Mrvoš-Sermek, D. Matković-Čalogović, J. Sabolović, *Cryst. Growth Des.* **2018**, *18*, 5138–5154.

[62] T. J. M. de Bruin, A. T. M. Marcelis, H. Zuilhof, E. J. R. Sudhölter, *Phys. Chem. Chem. Phys.* **1999**, *1*, 4157–4163.

[63] C. S. Tautermann, J. Sabolović, A. F. Voegele, K. R. Liedl, *J. Phys. Chem. B* **2004**, *108*, 2098–2102.

[64] J. G. Mesu, T. Visser, F. Soulimani, E. E. van Faassen, P. de Peinder, A. M. Beale, B. M. Weckhuysen, *Inorg. Chem.* **2006**, *45*, 1960–1971.

[65] K. M. Wellman, B. K. Wong, *Proc. Natl. Acad. Sci. USA* **1969**, *64*, 824–827.

[66] P. Deschamps, P. P. Kulkarni, B. Sarkar, *Inorg. Chem.* **2004**, *43*, 3338–3340.

[67] H. C. Freeman, J. Guss, M. J. Healy, R.-P. Martin, C. E. Nockolds, B. Sarkar, *Chem. Commun.* **1969**, 225–226.

[68] W.-Y. Wan, E. J. Milner-White, *J. Mol. Biol.* **1999**, *286*, 1633–1649.

[69] M. Pezzato, G. Della Lunga, M. C. Baratto, A. Sinicropi, R. Pogni, R. Basosi, *Magn. Reson. Chem.* **2007**, *45*, 846–849.

[70] G. Sciortino, G. Lubinu, J.-D. Maréchal, E. Garriba, *Magnetochemistry* **2018**, *4*, 55.

[71] T. H. Dunning Jr.,P. J. Hay in *Methods of Electronic Structure Theory, Modern Theoretical Chemistry, Vol. 3* (Ed.: H. F. Schaefer III), Plenum Press, New York, **1977**, pp. 1–28.

[72] M. J. Frisch, J. A. Pople, J. S. Binkley, *J. Chem. Phys.* **1984**, *80*, 3265–3269.

[73] T. Clark, J. Chandrasekhar, G. W. Spitznagel, P. v. R. Schleyer, *J. Comput. Chem.* **1983**, *4*, 294–301.

[74] P. J. Hay, W. R. Wadt, *J. Chem. Phys.* **1985**, *82*, 270–283.

[75] W. R. Wadt, P. J. Hay, *J. Chem. Phys.* **1985**, *82*, 284–298.

[76] P. J. Hay, W. R. Wadt, *J. Chem. Phys.* **1985**, *82*, 299–310.

[77] G. Scalmani, M. J. Frisch, *J. Chem. Phys.* **2010**, *132*, 114110/1–15.

[78] M. J. Frisch, G. W. Trucks, H. B. Schlegel, G. E. Scuseria, M. A. Robb, J. R. Cheeseman, G. Scalmani, V. Barone, B. Mennucci, G. A. Petersson, H. Nakatsuji, M. Caricato, X. Li, H. P. Hratchian, A. F. Izmaylov, J. Bloino, G. Zheng, J. L. Sonnenberg, M. Hada, M. Ehara, K. Toyota, R. Fukuda, J. Hasegawa, M. Ishida, T. Nakajima, Y. Honda, O. Kitao, H. Nakai, T. Vreven, J. A. Montgomery, Jr., J. E. Peralta, F. Ogliaro, M. Bearpark, J. J. Heyd, E. Brothers, K. N. Kudin, V. N. Staroverov, R. Kobayashi, J. Normand, K. Raghavachari, A. Rendell, J. C. Burant, S. S. Iyengar, J. Tomasi, M. Cossi, N. Rega, J. M. Millam, M. Klene, J. E. Knox, J. B. Cross, V. Bakken, C. Adamo, J. Jaramillo, R. Gomperts, R. E. Stratmann, O. Yazyev, A. J. Austin, R. Cammi, C. Pomelli, J. W. Ochterski, R. L. Martin, K. Morokuma, V. G. Zakrzewski, G. A. Voth, P. Salvador, J. J. Dannenberg, S. Dapprich, A. D. Daniels, Ö. Farkas, J. B. Foresman, J. V. Ortiz, J. Cioslowski, and D. J. Fox, GAUSSIAN 09 (Revision D.01), Gaussian Inc., Wallingford, CT, 2013.

[79] A. K. Rappe, C. J. Casewit, K. S. Colwell, W. A. Goddard III, W. M. Skiff, *J. Am. Chem. Soc.* **1992**, *114*, 10024–10035.

[80] F. Neese, *Wiley Interdiscip. Rev.: Comput. Mol. Sci.* **2012**, *2*, 73–78.

[81] F. Neese, *Wiley Interdiscip. Rev.: Comput. Mol. Sci.* **2018**, *8*, e1327.

[82] A. J. H. Wachters, *J. Chem. Phys.* **1970**, *52*, 1033–1036.

[83] T. Fujii, F. Moynier, M. Abe, K. Nemoto, F. Albarède, *Geochim. Cosmochim. Acta* **2013**, *110*, 29–44.

[84] J. P. Perdew, K. Burke, M. Ernzerhof, *Phys. Rev. Lett.* **1996**, *77*, 3865–3868.

[85] J. P. Perdew, K. Burke, M. Ernzerhof, *Phys. Rev. Lett.* **1997**, *78*, 1396.

[86] H.-J. Scholl, J. Hiittermann, *J. Phys. Chem.* **1992**, *96*, 9684–9691.